

## Evolution of Developmental Control Mechanisms

Neurogenesis in an annelid: Characterization of brain neural precursors in the polychaete *Capitella* sp. I

Néva P. Meyer, Elaine C. Seaver\*

Kewalo Marine Laboratory, Pacific Biosciences Research Center, University of Hawaii, 41 Ahui Street, Honolulu, HI 96813, USA

## ARTICLE INFO

## Article history:

Received for publication 7 January 2009

Revised 11 June 2009

Accepted 12 June 2009

Available online 21 June 2009

## Keywords:

Brain

Polychaete

*Capitella* sp. I

Proneural

Annelid

Lophotrochozoan

Ingression

*Achaete-scute*

Neurogenesis

*elav*

## ABSTRACT

Intertaxonomic comparisons are important for understanding neurogenesis and evolution of nervous systems, but high-resolution, cellular studies of early central nervous system development and the molecular mechanisms controlling this process in lophotrochozoans are still lacking. We provide a detailed cellular and molecular description of early brain neurogenesis in a lophotrochozoan annelid, *Capitella* sp. I. We utilized different approaches including Dil lineage tracing, immunohistochemistry, BrdU labeling, and gene expression analyses to characterize neural precursor cells in *Capitella* sp. I. Brain neurogenesis proceeds by the ingression of single cells from the anterior ectoderm to generate a stratified epithelial layer. Most cell divisions are restricted to apically localized cells with mitotic spindles oriented parallel to the epithelial layer. Prior to and during this process, an *achaete-scute* complex homolog, *Cap1-ash1*, is expressed in clusters of surface cells in the anterior ectoderm, consistent with a proneural function for *Cap1-ash1*. In contrast, a homolog of the neural differentiation marker *elav*, *Cap1-elav1*, is restricted to basally localized cells within the forming brain. Unlike insects, *Capitella* sp. I does not have morphologically obvious enlarged neuroblasts, although *Capitella* sp. I brain neurogenesis displays several similarities with non-insect arthropod and vertebrate neurogenesis, providing a useful lophotrochozoan model for comparison.

© 2009 Elsevier Inc. All rights reserved.

## Introduction

A key step during early central nervous system (CNS) development is fate specification of neural precursor cells (NPCs), which generate the brain and nerve cord. Although there are striking anatomical and organizational differences in the CNS among various bilaterian phyla, one major commonality is that NPCs usually originate from the ectoderm. Because the CNS is an internal organ in many bilaterians, or at least subepidermal, NPCs must be internalized and/or segregated from presumptive epidermal cells. Additionally, NPCs must expand in number and restrict their fate to generate the wide variety of neurons that constitute the CNS. Most of our detailed understanding of neurogenesis comes from studies in two of three bilaterian superclades, the deuterostomes (e.g., vertebrates) and the ecdysozoans (e.g., arthropods). At first glance, the well-characterized cellular mechanisms of NPC internalization in arthropods and vertebrates appear quite different. In vertebrates, NPCs are localized to the dorsal ectoderm and are internalized as a sheet of cells to form the neural tube (Jacobson and Rao, 2005; Mathis et al., 2001). After neural tube closure, NPCs divide at the apical surface of the neuroepithelium, then move basally as their progeny exit the cell cycle and differentiate into neurons (Jacobson and Rao, 2005; Merkle and Alvarez-Buylla, 2006). During insect embryogenesis, NPCs, or neuroblasts, are localized to

the ventral ectoderm and internalize as single cells by ingression, which begins with constriction of the apical membrane (bottle-cell formation) and is followed by detachment from the apical surface of the epithelium (Doe and Goodman, 1985a; Hartenstein and Campos-Ortega, 1984). After internalization, neuroblasts divide asymmetrically and their progeny generate the CNS (Doe, 1992; Doe et al., 1998).

Recent data describing neurogenesis in spiders and myriapods (e.g., centipedes) have provided new hypotheses of possible neurogenic ground patterns within the arthropods. In spiders and myriapods, groups of mitotically quiescent NPCs are internalized through bottle-cell formation and subsequent apical detachment to form part of the CNS (Dove and Stollewerk, 2003; Stollewerk and Simpson, 2005; Stollewerk et al., 2001). After all NPCs have detached, epidermal cells overgrow the remaining surface neuroectoderm, which forms the rest of the CNS (Chipman and Stollewerk, 2006; Dove and Stollewerk, 2003; Stollewerk, 2002). This contrasts with insect and vertebrate neurogenesis in which substantial NPC expansion occurs after internalization. However, the later phase is similar to vertebrate neurogenesis, in which the entire neural plate is internalized to form the CNS.

Despite differences in the cellular mechanisms of neurogenesis, vertebrates and arthropods both utilize proneural, basic helix–loop–helix (bHLH) gene family members and Notch/Delta lateral inhibition to regulate NPC formation. In chick and mouse embryos, NPCs are maintained in a stem cell state by fibroblast growth factor (FGF) and uniform Notch/Delta signaling (Diez del Corral et al., 2002; Hammerle

\* Corresponding author.

E-mail address: [seaver@hawaii.edu](mailto:seaver@hawaii.edu) (E.C. Seaver).

and Tejedor, 2007; Mathis et al., 2001; Yoon and Gaiano, 2005). In mouse and *X. laevis* embryos, expression of proneural genes of the *achaete-scute* complex (*asc*) and other proneural gene families (e.g., *neurogenin*) result in fate specification of NPCs and a concomitant decrease in their mitotic potential, often through upregulation of *delta* expression (Bertrand et al., 2002; Casarosa et al., 1999; Chitnis and Kintner, 1996; Yoon and Gaiano, 2005). In *D. melanogaster*, small clusters of neuroectoderm cells express proneural *asc* genes (*Isc*, *ac*, *sc*), with the presumptive neuroblast expressing the highest level of *asc* genes (Cabrera et al., 1987; Martin-Bermudo et al., 1991; Skeath and Carroll, 1992), whose protein products upregulate *delta* expression. Delta activates the Notch receptor in surrounding cells, resulting in a downregulation of *asc* expression and acquisition of an epidermal fate (Heitzler and Simpson, 1991; Kunsch et al., 1994; Skeath and Carroll, 1992; Skeath and Thor, 2003). The molecular mechanisms involved in NPC specification in spiders and myriapods are similar to those found in insects, including the use of *Asc* homologs and Notch/Delta lateral inhibition (Stollewerk, 2002; Stollewerk and Simpson, 2005; Stollewerk et al., 2001).

A huge gap remains in our knowledge of CNS development in the third bilaterian clade, the lophotrochozoans. In the mollusk *Aplysia californica*, NPCs reside in ectodermal proliferative zones and migrate from the epithelial layer individually or in small clusters to form ganglia, where they are mitotically quiescent (Jacob, 1984). In annelids, neurogenesis is well-characterized in the leech ventral nerve cord, which is generated by ectodermal stem cells known as the N, O, P and Q teloblasts. These cells divide asymmetrically along the anteroposterior axis to produce a linear column of progeny, producing both epidermal and neural derivatives, with the N teloblast producing the majority of CNS neurons by local proliferation (Kramer and Weisblat, 1985; Shankland, 1995; Torrence and Stuart, 1986). In the polychaete annelid, *Platynereis dumerilii*, molecular markers expressed at different stages of neurogenesis in the developing ventral nerve cord have recently been reported (Denes et al., 2007; Simionato et al., 2008). Interestingly, proneural bHLH genes, including an *asc* homolog, are expressed in the ventral neuroectoderm, suggesting a possible proneural function in a lophotrochozoan (Simionato et al., 2008). Despite these descriptions, high-resolution, cellular studies of early neurogenesis and characterization of the molecular mechanisms controlling fate specification and internalization of NPCs in lophotrochozoans are still lacking.

We have begun our investigation of neurogenesis in the annelid *Capitella* sp. I by focusing on brain development and addressing the following questions: 1) from where in the embryo do brain NPCs arise? 2) How are brain NPCs internalized from the ectoderm? 3) What are the cell division and neural differentiation patterns that generate the population of neurons in the brain? 4) Are *asc* homologs expressed at the correct time and place to be involved in NPC fate specification and/or internalization in *Capitella* sp. I?

## Materials and methods

### Animal care

A laboratory colony of *Capitella* sp. I was maintained as described in Seaver et al. (2005). Animals were kept in 20  $\mu$ m filtered seawater (FSW) at 19 °C. Embryos and larvae were collected as previously described (Seaver et al., 2005).

### Dil labeling

~280  $\mu$ g/ $\mu$ L DiI (1,1'-dioctadecyl-3,3,3',3'-tetramethylindocarbocyanine perchlorate; DiI<sub>C18</sub>(3), Molecular Probes) in ethanol was loaded into borosilicate, filament needles and then ionophoretically introduced into cell membranes for 15–45 s using a box powered with 9 V through a 1 M $\Omega$  resistor (Birgbauer and Fraser, 1994). This

technique allows DiI to cross the egg membrane and become incorporated into small patches of 1–7 surface cells (usually 1–3). After labeling, animals were fixed (see below) every few hours at 19 °C and then incubated overnight at 4 °C in 1:200 BODIPY FL-phalloidin or Alexa Fluor 488-phalloidin (Molecular Probes) in phosphate buffered saline (PBS), rinsed 3–4 times in PBS, incubated in 80% glycerol in PBS plus 0.125  $\mu$ g/mL BisBenzimide Hoechst 33342 (Sigma) for 3–12 h at 4 °C and then analyzed. For confocal imaging, animals were incubated overnight at 4 °C in 1:1000 TO-PRO-3 iodide (Molecular Probes) and 1:200 BODIPY FL-phalloidin in PBS, rinsed 3–4 times in PBS, then incubated in SlowFade Gold (Molecular Probes) for 3 h at 4 °C and analyzed. Some animals were imaged live. The initial point of DiI application could often be seen as a small spot in the egg membrane even 3 days after labeling (Figs. S1A–A', C–E', Figs. 2D–E').

### BrdU labeling

Stages 3–9 animals were incubated in 0.1 mg/mL BrdU (5-bromo-2'-deoxyuridine, Sigma) in FSW for 30 min at r.t. and then immediately fixed (see below). Incorporation of BrdU was visualized according to Seaver et al. (2005), except that a fluorescently-conjugated secondary antibody was used.

### Fixation

Prior to fixation, animals were pretreated as follows: 1) stages 1–3 embryos were incubated for 3 min at r.t. in a 1:1 mixture of fresh 1 M sucrose and 0.25 M sodium citrate, mixed immediately before addition to animals. This was followed by 3 FSW washes. 2) Stages 4–9 larvae were relaxed for 5–10 min at r.t. in a 1:1 mixture of 0.37 M MgCl<sub>2</sub> and FSW. The five fixation methods used are as follows: 1) DiI-labeled animals were fixed in 3.7% formaldehyde and 0.05 M EDTA in FSW for 1 h at r.t. and then washed in PBS. 2) Animals to be labeled with the anti- $\beta$ -tubulin antibody were fixed at r.t. for 90 s in 0.2% glutaraldehyde and 4% paraformaldehyde (Electron Microscopy Sciences) in PBS and then for 1 h in 4% paraformaldehyde in PBS. This was followed by several washes in PBS + 0.1% Triton X-100 (PBT). 3) After BrdU labeling, animals were fixed in 3.7% formaldehyde in FSW for 30 min at r.t. and then washed in PBS. 4) For all other antibody labeling, animals were fixed at r.t. for 15 min in 3.7% formaldehyde in FSW and then for 7 min in 3.7% formaldehyde and 0.05% Tween-20 in FSW. This was followed by several washes in PBT. 5) In situ hybridization, animals were fixed for either 6 h at r.t. or overnight at 4 °C in 3.7% formaldehyde in FSW, followed by several PBS washes and dehydration in methanol.

### Antibody/phalloidin staining

Animals were incubated in block consisting of PBT + 10% heat-inactivated goat serum (Sigma) for 1 h at r.t. and then in primary antibody in block overnight at 4 °C. Following several r.t. PBT washes, animals were incubated in secondary antibody in block for either 3 h at r.t. or overnight at 4 °C. Animals were then washed with several exchanges of PBT for a few hours at r.t. or overnight at 4 °C. After PBT washes, 1:200 BODIPY FL-phalloidin or Alexa Fluor 488-phalloidin in PBT was added for 3 h at r.t. This was followed by 4 PBS washes at r.t. over 1 h.

For imaging, animals were cleared by one of two methods. For most specimens, animals were incubated in 80% glycerol in PBS plus 0.125  $\mu$ g/mL Hoechst for 3 h up to a few days at 4 °C. Alternatively, animals in Figs. 5 and 6 and the pHist labeled animals in Fig. 7 were rinsed 3 times in PBS, 2 times in H<sub>2</sub>O, dehydrated with 30%, 60%, 90%, and 2 $\times$  100% 2-propanol washes over a total of 7 min, mounted in 2:1 benzyl benzoate: benzyl alcohol (Sigma), and immediately analyzed.

Primary antibodies used are as follows: 1:4 mouse anti- $\beta$ -tubulin (E7 supernatant; Developmental Studies Hybridoma Bank developed

under the auspices of the NICHD and maintained by The University of Iowa, Dept. of Biological Sciences, Iowa City, IA), 1:800 mouse anti-acetylated-tubulin (6-11B-1, Sigma), 1:500 mouse anti-histone (F152, C25.WJJ, Millipore), 1:200 rabbit anti-phospho-histone H3 (Millipore), 1:50 mouse anti-BrdU (B44, Becton Dickinson) and 1:400 rabbit anti-5-HT (ImmunoStar). Secondary antibodies used are as follows: 1:400 goat anti-mouse or anti-rabbit FITC, 1:400 goat anti-mouse or anti-rabbit Rhodamine, and 1:1000 donkey anti-mouse or anti-rabbit Alexa Fluor 647 (Molecular Probes).

#### BrdU and pHist graphs

For measurements and graphing of BrdU<sup>+</sup> and pHist<sup>+</sup> nuclei, see [Supp. materials and methods](#).

#### Gene isolation and orthology analyses

See [Supp. materials and methods](#).

#### Whole mount in situ hybridization

mRNA detection was carried out using previously published protocols (Seaver and Kaneshige, 2006; Seaver et al., 2001). Animals were hybridized 72 h at 65 °C with 1 ng/μL of each probe except for the short *Capl-ash1* probe and the *Capl-ash2* probe, which were hybridized at 2 ng/μL.

#### Microscopy

Confocal imaging was performed using a LSM 510 confocal microscope (Zeiss). 3D-reconstructions were generated using either the LSM 510 software or ImageJ (NIH). Live and fixed DiI-labeled animals were imaged using an Axioskop 2 plus with an AxioCam HRm camera (Zeiss) and Openlab software version 4.0.1 (Improvision). After in situ hybridization, animals were photographed using an Axioskop

mot plus (Zeiss) coupled with a 3.34 megapixel Cool-Pix 990 digital camera (Nikon).

## Results

### Brain development in *Capitella* sp. I

*Capitella* sp. I embryos develop by spiral cleavage to generate non-feeding larvae. The entire process from fertilized egg to metamorphosis takes ~9 days at 19 °C, and the developmental staging system progresses from stages 1 to 9. Each stage corresponds to approximately one day of development and is defined by appearance of a specific set of morphological features (Seaver et al., 2005). Embryos gastrulate by epiboly (stage 3), and four days later (stage 7), larvae have a segmented trunk positioned between two ciliary bands (prototroch and telotroch) and a CNS comprised of brain and ventral nerve cord (Fig. 1A). Brain development in *Capitella* sp. I begins near the end of gastrulation with a thickening of the anterior ectoderm (stage 3, Figs. 1B, D, false-colored pink). At this stage, the thickening is bilaterally uniform (Fig. 1B), but by the end of stage 4, two presumptive lobes are apparent (Fig. 1E and not shown). These lateral, ectodermal thickenings continue to increase in size through stage 5 (Figs. 1C, F), and by late stage 6, the brain, or cerebral ganglion, has two distinct lobes comprised of approximately 500 cells in total. At this stage, the brain appears morphologically separate from the overlying epidermis, which coincides with muscle formation between the epidermis and brain (Fig. 1G). The brain continues to enlarge slightly, change shape, and separate from the epidermis during stages 7–9 (Figs. 1H–J). In juveniles that have recently undergone metamorphosis, the brain is similar in size and shape to the brain in stage 9 larvae (compare Fig. 1K with J).

### Anterior ectodermal cells contribute to the brain

To determine the temporal and spatial origin of brain NPCs in *Capitella* sp. I, we labeled small clusters of anterior ectodermal cells in

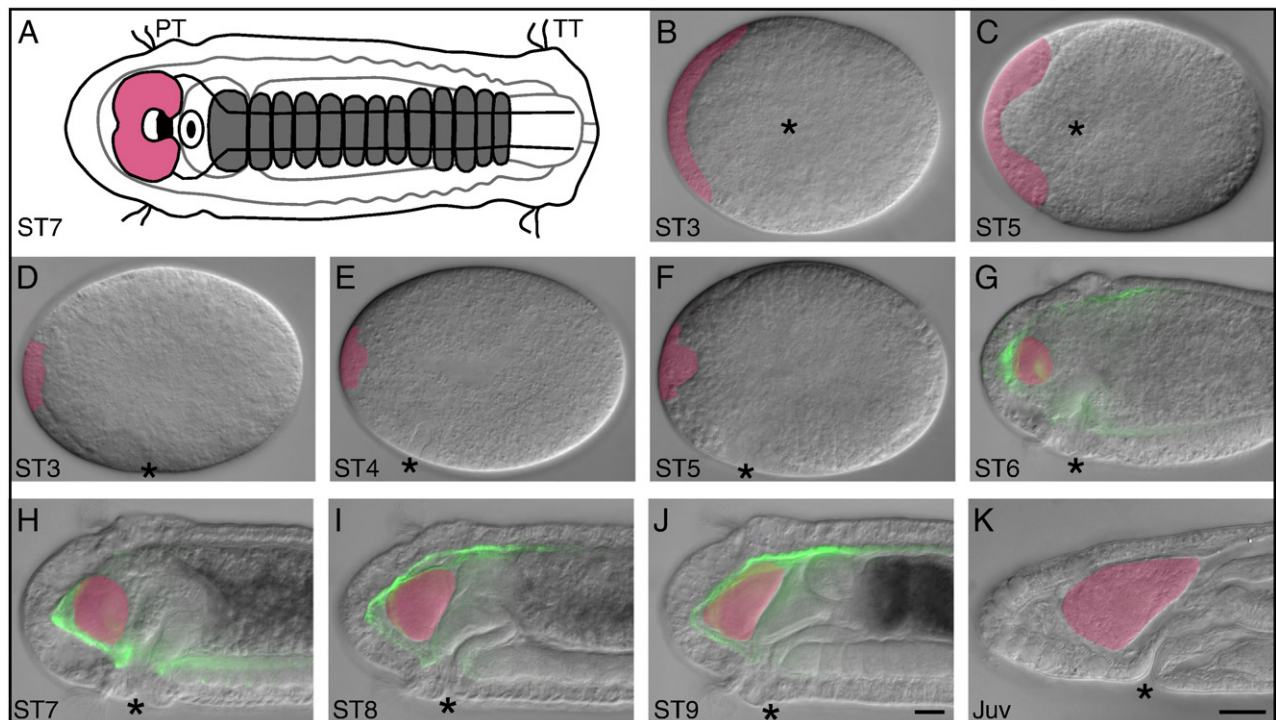


**Fig. 1.** Brain development in *Capitella* sp. I. (A) Diagram of the brain (pink) and ventral nerve cord (grey) of a stage 7 larva. The prototroch (PT) and telotroch (TT) are indicated. (B–K) DIC images of the developing brain (false-colored pink). Images in G–J are DIC images overlaid with green epifluorescent images of phalloidin staining at the same focal plane to highlight muscle fibers. A–C are ventral views, anterior to the left; D–K are lateral views, anterior to the left, ventral down. An asterisk marks the position of closing blastopore in B and D and the mouth in C and E–K. The stage of the animal is depicted in the lower left corner of each image. Scale bars in J and K are 25 μm; B–J are to the same scale.

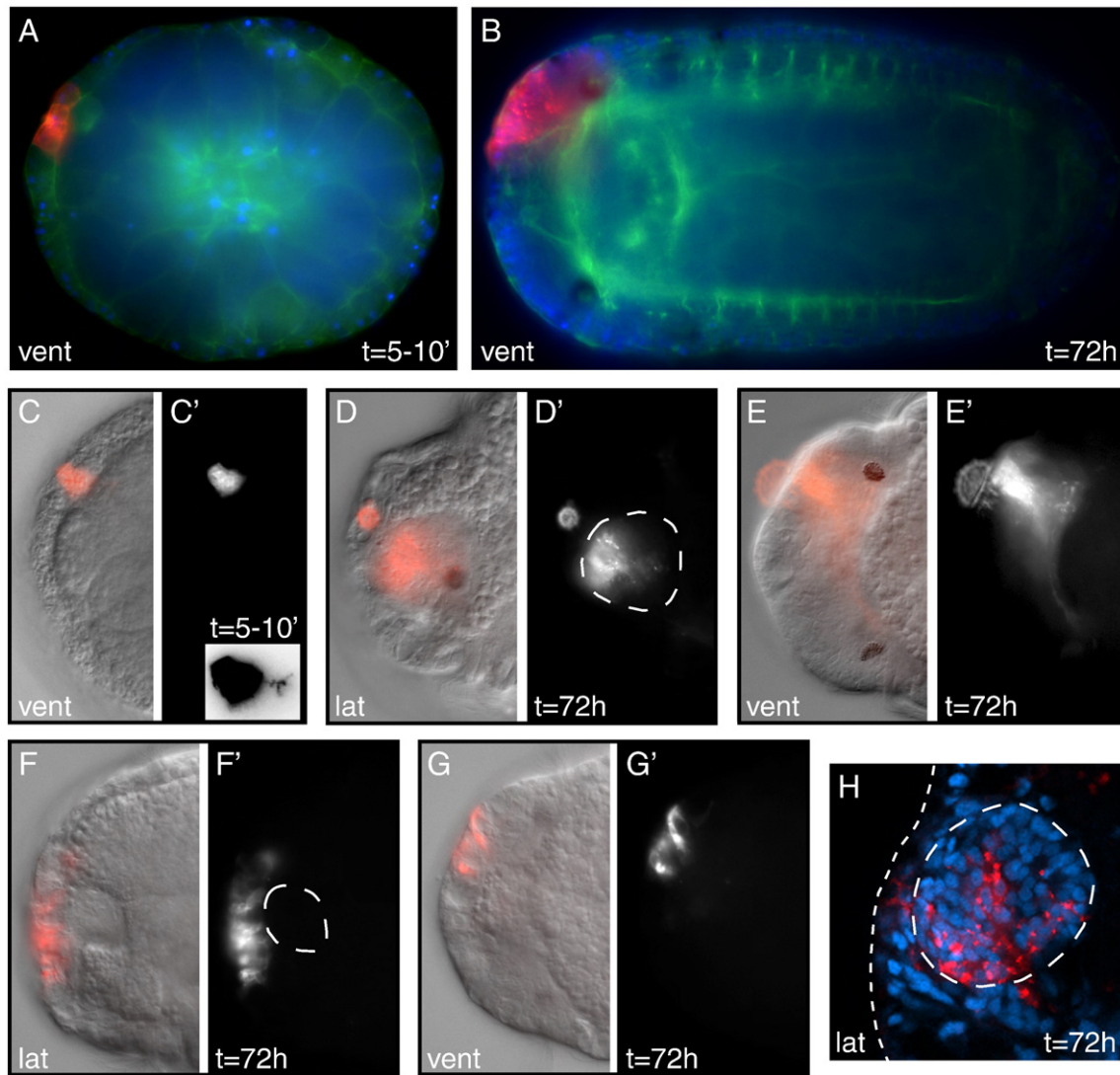


**Fig. 2.** Stage 3 anterior ectodermal cells contribute to the brain. (A, C–C') Stage 3 animals immediately after labeling the anterior ectoderm with Dil. (B, D–H) Stage 6 animals ~72 h after Dil labeling the anterior ectoderm at stage 3. Images A and B are merged epifluorescent images of Dil (red), phalloidin (green) and Hoechst (blue). Images C, D, E, F, and G are DIC images overlaid with red Dil epifluorescent images taken at the same focal plane. Images C', D', E', F' and G' are single-channel epifluorescent images of Dil labeling. The image in H is a stack of confocal micrographs of Dil (red) and the nuclear stain TO-PRO-3 (blue). Inset in C' is an inverted, 1.2 $\times$  magnification of C' showing a basal process extending from the labeled cell. The dashed line in D', F' and H delineates one lobe of the brain. The vertical, dashed line in H delineates the outer edge of the epidermis. In A–H, the view is indicated on the lower left (lat, lateral; vent, ventral), and the time after labeling is indicated on the lower right of each image or pair of images. In all lateral views, anterior is to the left and ventral down; in all ventral views, anterior is to the left. Images labeled with the same letter correspond to the same focal plane of one animal. Images in D–E' are of the same animal.

stage 3 animals and followed their fate using the lipophilic dye Dil. Because more than one cell is often labeled, we refer to their descendants as polyclones. At the initial time of labeling, Dil is confined to a few surface ectodermal cells and does not spread into the underlying, yolky endodermal cells (Figs. 2A, C–C', Figs. S1A–B"). Labeled cells are large, cuboidal, and fairly uniform in size and shape. These cells often have basal processes that extend between adjacent endoderm cells (Fig. 2C', inset), along the interface between ectoderm and endoderm cells, or even from the lateral surface of ectodermal cells (not shown). Three days (stage 6) after labeling, two categories of Dil<sup>+</sup>

polyclones are observed: those with epidermis and brain labeled (62%, Table 1, first column; Figs. 2B, D–E', H, Figs. S1C–G) and those with epidermis alone labeled (38%; Figs. 2F–G'). In all animals with Dil<sup>+</sup> cells in the brain, the epidermis is also labeled (Table 1, second column). Labeling the anterior ectoderm outside of the region of the ectodermal thickening results in epidermal-only, Dil<sup>+</sup> polyclones. Within the brain, Dil<sup>+</sup> cells are often contiguous (Fig. 2H, Figs. S1C, C', E, E') and confined to either the left or the right lobe (Figs. 2E, E', Figs. S1D, D'). We find polyclones in all regions of the brain. Occasionally, labeled cells are positioned separate from the bulk of the polyclone,

**Table 1**  
Final position and size of Dil polyclones in animals labeled at stages 3–5.

Stage labeled	% polyclones with Dil in brain	% Dil <sup>+</sup> brain polyclones with Dil in epidermis	% brain labeled				
			1%	2–10%	11–20%	21–30%	>30%
ST3	62 (31/50)	100 (30/30)	3 (1/31)	35 (11/31)	55 (17/31)	6 (2/31)	0 (0/31)
ST4	49 (24/49)	96 (23/24)	50 (12/24)	33 (8/24)	17 (4/24)	0 (0/24)	0 (0/24)
ST5	30 (24/81)	100 (24/24)	58 (14/24)	25 (6/24)	17 (4/24)	0 (0/24)	0 (0/24)

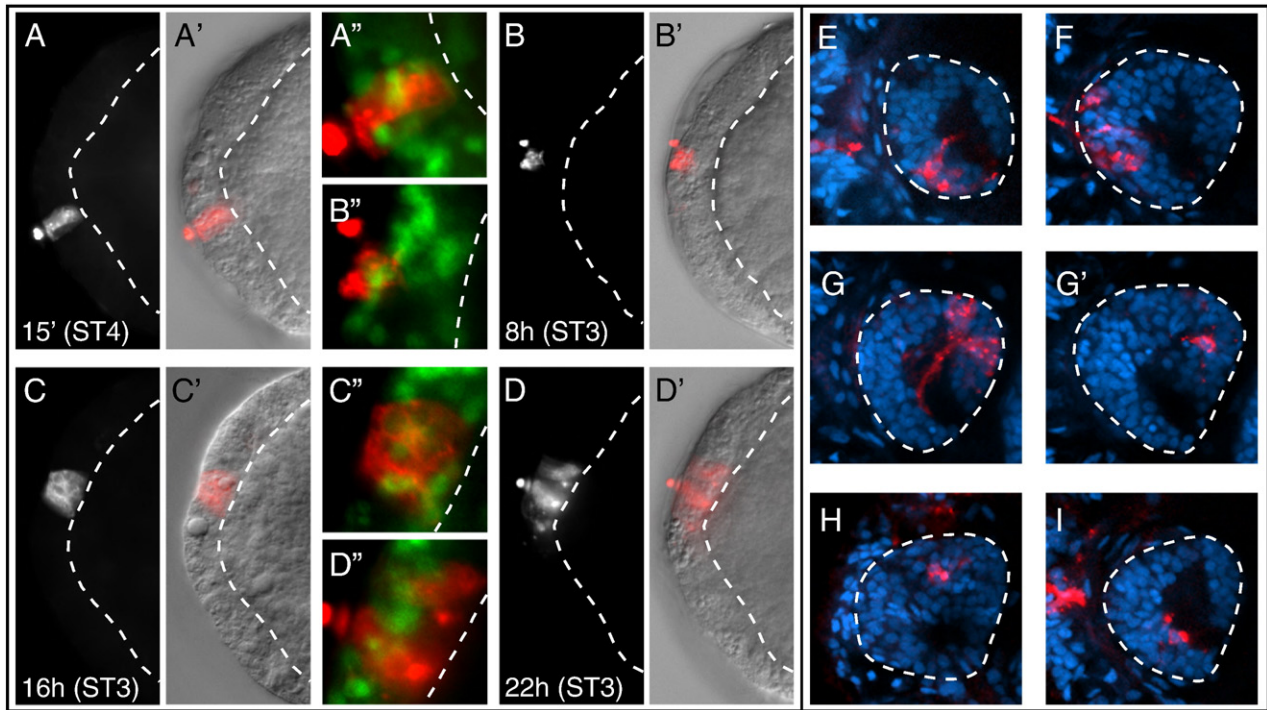


**Fig. 3.** Analysis of Dil polyclones at various time points after labeling stage 3 and 4 animals. (A–D') Time points from 15 min to 22 h after labeling the anterior ectoderm with Dil. (E–I) Stacks of confocal micrographs through the brain of stage 7 animals ~72 h after Dil (red) labeling the anterior ectoderm at stage 4. Animals were stained with TO-PRO-3 (blue) to highlight nuclei. In A–D', images labeled with the same letter correspond to the same focal plane of a single animal. G and G' are confocal micrograph stacks at different depths through the same animal. The labels in A–D correspond to the time after labeling followed in parentheses by the stage at which the animal was labeled. Images A, B, C and D are single-channel epifluorescence images of Dil labeling. Images A', B', C' and D' are DIC images overlaid with red Dil epifluorescent images taken at the same focal plane. Images A'', B'', C'' and D'' are merged epifluorescent images of Hoechst (green) and Dil (red). Dashed line in A–D' delineates the basal edge of the anterior ectodermal thickening. In E–I the dashed line delineates one brain lobe. Images A–D' are ventral views, anterior to the left; E–I are lateral views, anterior to the left, ventral down.

indicating mixing between labeled and unlabeled cells (Fig. S1G, arrows). Brain polyclone sizes range from a few cells to 10–30% of the entire brain (compare Figs. S1F, F' with Figs. S1E, E'), although in most cases ~12% of the brain (50 cells) is labeled (Table 1; Figs. 2E, E', Figs. S1E, E'). We do not see labeled cells in the ventral nerve cord ( $n = 50$  animals). These results demonstrate that in *Capitella* sp. I, brain NPCs are localized to the anterior ectodermal thickening at stage 3.

To determine the time period of NPC contribution to the brain, the anterior ectoderm was also labeled with Dil at stages 4 and 5. Immediately after labeling at stage 4, Dil<sup>+</sup> cells that span the epithelium (Figs. 3A–A'') and/or surface cells that do not extend to the basal edge of the epithelium (similar to Figs. 3B–B'') can be seen. Many cells that span the epithelium at stage 4 have a columnar shape, which contrasts with the cuboidal-shaped cells present at stage 3 (compare Figs. 3A–A' with Figs. 2A, C, C'). Two to three days later, two categories of Dil<sup>+</sup> polyclones are observed: those with epidermis and brain labeled (49%, Table 1; Figs. 3E–I) and those with epidermis alone labeled (51%). The percentage of animals with Dil<sup>+</sup> brain cells is lower in animals labeled at stage 4 than in animals labeled at stage 3 (49% versus 62%, respectively, Table 1). In addition, Dil<sup>+</sup> polyclones in the brain are generally smaller in animals labeled at stage 4 (Table 1; Figs. 3E–I) than in those labeled at stage 3 (Table 1; Fig. 2H). There is some mixing between labeled and non-labeled cells (Figs. 3F, G, G'). For example, Figs. 3G and G' are different focal planes of the same brain lobe showing a labeled cell apart from the bulk of the polyclone. Similar to stage 3, brain polyclones in animals labeled at stage 4 are confined to the left or right lobe.

Immediately after labeling stage 5 animals, Dil is confined to a few surface cells that do not span the anterior ectodermal thickening (Figs. 4A, C, C', Figs. S2A–B'). These cells are generally smaller than cells labeled at stage 3 (compare Fig. 2A with Fig. 4A). Two days later (stage 7), Dil<sup>+</sup> polyclones are predominantly limited to the epidermis (70%; Figs. 4B, D, D', Figs. S2C–E'). The remaining polyclones include

labeled cells in both the epidermis and the brain, although the polyclones in the brain are small (58% with 1% brain labeled, Table 1; Figs. 4E–H, Figs. S2F, F'). The distribution of polyclone sizes within the brain is similar to animals labeled at stage 4, and there is some mixing between labeled and non-labeled cells (Figs. 4E–F). For example, Figs. 4E and E' are different focal planes of the same brain lobe, showing a Dil<sup>+</sup> cell separate from the bulk of the polyclone. Thus, the anterior ectoderm continues to contribute to the brain at stage 5, but to a lesser extent than at stage 3. Furthermore, while some polyclones expand from stage 5 to stage 7 (Figs. S2C–E'), others do not and still contain only 1–7 cells (Figs. 4D, D'). This suggests that by stage 5, only a subset of anterior ectodermal cells is dividing. These Dil labeling results demonstrate that in *Capitella* sp. I, brain NPCs reside in the anterior ectoderm and can contribute to the brain from stage 3 through at least stage 5, although this capacity is greatly reduced over time.

To determine how polyclones expand and contribute to the brain, animals were examined at intermediate time points after labeling the anterior ectoderm with Dil at stages 3 and 4. In general, the progeny of labeled cells remain in close proximity to one another as the epithelium thickens and polyclones increase in cell number over time (Figs. 3C–C''). In the first 12 h after labeling, Dil<sup>+</sup> cells usually span the apical–basal width of the ectoderm, and cells in a polyclone often only double in number (not shown). After 12 h, the number of Dil<sup>+</sup> cells gradually increases, generating larger polyclones comprised of smaller cells (Figs. 3C'', D''). In a small subset of polyclones, labeled cells interspersed with unlabeled cells are visible within ~20 h of labeling (Figs. 3D–D''). In general, no labeled cells are seen posterior to the prototroch.

#### *Presumptive brain NPCs are internalized by ingression as single cells*

After determining that brain NPCs originate from the anterior ectoderm in *Capitella* sp. I, we next examined their mode of

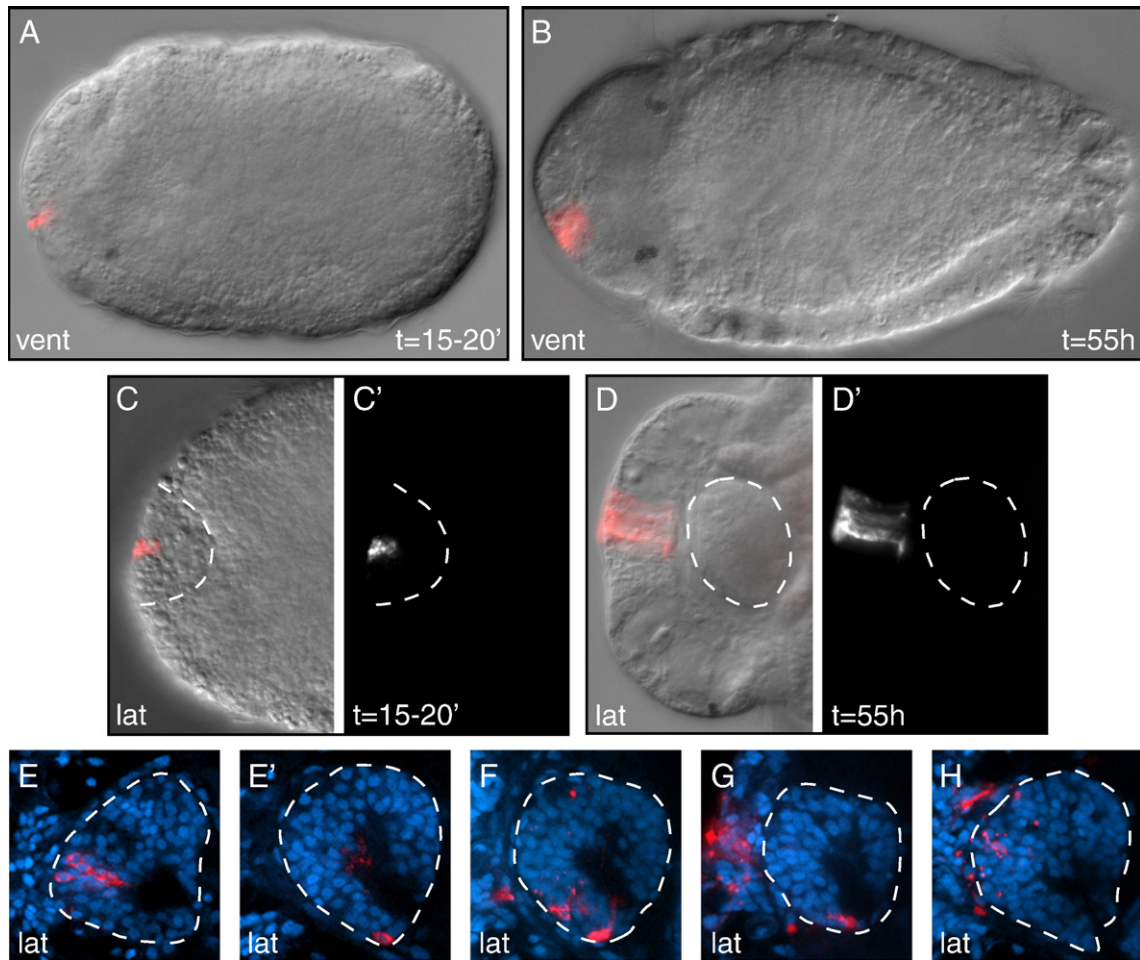


**Fig. 4.** Stage 5 anterior ectoderm predominantly generates epidermis. (A, C, C') Stage 5 animals immediately after labeling the anterior ectodermal thickening with Dil. (B, D–H) Stage 7 animals ~55 h after Dil labeling the anterior ectoderm at stage 5. Images A–C and D are DIC images overlaid with red Dil epifluorescent images taken at the same focal plane. Images C' and D' are single-channel, epifluorescent images of Dil labeling. Images E–H are stacks of confocal micrographs of Dil (red) and the nuclear stain TO-PRO-3 (blue). A dashed line delineates the anterior ectodermal thickening in C and C' and one brain lobe in D–H. The view in A–H is indicated in the lower left (lat, lateral; vent, ventral). In A–D', time after labeling is indicated in the lower right of each image or pair of images. In all lateral views, anterior is to the left and ventral down; in all ventral views, anterior is to the left.

internalization. In other animals, NPCs are internalized by different cellular mechanisms, including cell divisions oriented perpendicular to the epithelial plane, invagination, and ingression (Jacobson and Rao, 2005; Skeath and Thor, 2003; Stollewerk and Simpson, 2005). We use the term ingression to refer to the process of single or small groups of cells undergoing bottle-cell formation and subsequently detaching from the apical face of the epithelial layer. These cells can either remain within or migrate out of the epithelium. To determine how *Capitella* sp. 1 brain NPCs are internalized, we analyzed the morphology of individual cells in the anterior ectoderm from stage 3 through 4 (Fig. 5). During stage 3, when a blastopore is still visible, the anterior ectoderm is a simple epithelium comprised of a single layer of large, cuboidal cells (Figs. 5A–D; e.g., orange cell in D). From the end of gastrulation through stage 4, the anterior ectoderm transitions to a stratified epithelium that is up to 4 cells thick (Figs. 5I–M, P–W). However, the epithelium is not uniformly stratified, and single cells that span the entire apical–basal width of the epithelium can still be seen (closed arrowheads in Figs. 5I–L, Q–T, W; orange cells in L, T).

As the anterior ectoderm transitions to a stratified epithelium, cells with a bottle-cell morphology are observed (Fig. 5, arrowheads). At stage 3, the majority of anterior ectodermal cells have apically localized nuclei (Figs. 5A, C, D). As gastrulation progresses, cells with either basally shifted nuclei (Figs. 5E, F, arrowheads) or basally shifted nuclei and apically constricted membranes (arrowheads in Figs. 5B–D, G, H; pink cell in D) can be seen. These characteristics are

indicative of beginning bottle-cell formation and advanced bottle-cell formation, respectively. The basal edge of each bottle cell usually appears flush with the basal edge of the epithelium (Figs. 5E, G, H, arrowheads), indicating that these cells are not exiting the epithelial layer. We do not observe bottle cells at earlier stages (mid- and late-epiboly). After gastrulation through stage 4, the anterior ectoderm of a single animal contains multiple bottle cells (arrowheads in Figs. 5I–N, Q–V; pink cells in L, T). Bottle cells are often in close proximity to one another, sometimes within 1–3 cell diameters (Fig. 5V, arrowheads). We consider these cells to be ingressing as single cells because adjacent cells do not have a bottle-cell morphology. In the animals shown in Figs. 5K and S, there are two bottle cells separated by one non-bottle cell at slightly deeper focal planes (see Figs. 10B, C). Bottle cells are also occasionally seen in Dil labeling experiments (Fig. 5X, arrowhead). In addition to bottle cells, we see basally positioned cells that have completely detached from the apical side of the epithelial layer and have a flattened, or squamous, morphology (filled arrowheads in Figs. 5I–L, O, Q–T, W; turquoise cells in L, T). These are likely cells that remain within the epithelial layer after ingressing. The presence of bottle cells in the anterior ectoderm while surface cells are contributing to the brain suggests that brain NPCs are internalized by ingression as single cells.

In some animals, NPCs are internalized by cell divisions oriented perpendicular to the plane of the epithelium (Skeath and Thor, 2003). To determine whether this mechanism contributes to internalization

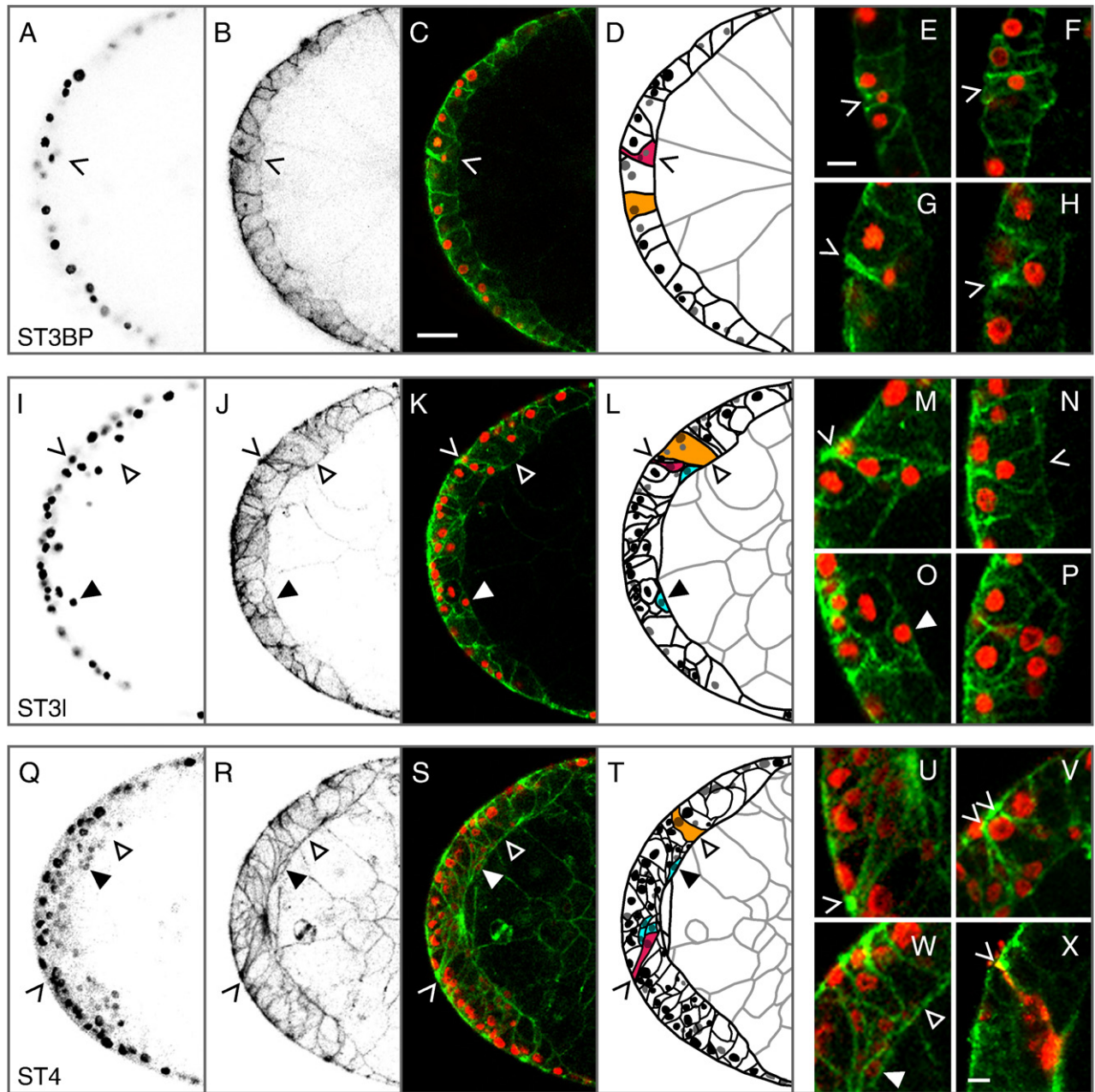


**Fig. 5.** Brain NPCs internalize by ingression. Confocal micrographs of the anterior ectodermal thickening towards the end of gastrulation (A–C, E–H, ST3BP), at the end of stage 3 (I–K, M–P, ST3I), and at stage 4 (Q–S, U–X, ST4). A, I and Q are single-channel, inverted, epifluorescent images of anti-histone staining. B, J and R are single-channel, inverted epifluorescent images of phalloidin staining. C, E–H, K, M–P, S and U–W are merged, epifluorescent images of anti-histone (red) and phalloidin (green) staining. D, L and T are traced diagrams of C, K and S, respectively. The image in X is of a stage 4 animal ~24 h after Dil labeling the anterior ectoderm. The animal was counter-stained with phalloidin (green), and an arrowhead points to a Dil-labeled bottle cell (red). Images A–F; I–O; Q–W are each from the same animal; A–C and G, I–M and O, and Q–U and W are the same confocal stack or slice. Bottle cells are indicated with arrowheads. Detached, squamous cells are indicated with filled arrowheads. Cells that span the epithelium are indicated with closed arrowheads. In the diagrams, nuclei in the plane of focus are black, nuclei out of the plane of focus are grey, examples of bottle cells are pink, detached squamous cells are turquoise, and cells that span the epithelium are orange. Images A–D, F–H and X are ventral views, anterior to the left. Images E and I–W are dorsal views, anterior to the left. The scale bar in C is 25  $\mu\text{m}$ ; A–D, I–L and Q–T are to the same scale. The scale bars in E and X are 5  $\mu\text{m}$ . E–H, M–P and U–W are to the same scale.

of brain NPCs in *Capitella* sp. 1, mitotic spindle orientation in the anterior ectodermal thickening was examined at stage 3. During mid-epiboly, prior to cell ingression, most mitotic spindles are oriented parallel to the plane of the epithelium (23 parallel, 2 oblique, and 0 perpendicular telophase spindles;  $n=9$  animals). Similarly, from late gastrulation to the end of stage 3, most spindles are oriented parallel to the epithelial plane (Figs. 6B, C, arrowheads; D). During metaphase, oblique spindles are present (Figs. 6A, arrowhead; D), but by telophase, the majority of spindles are oriented parallel to the epithelial plane (90%; Figs. 6C, arrowhead; D). To visualize the positions of dividing cells across the surface anterior ectoderm, a

confocal image of a stage 3 embryo is shown from an anterior view (Fig. 6E). The majority of spindles in the anterior ectoderm of this animal are parallel to the plane of the epithelium; only one is slightly oblique (Fig. 6F, arrow). Eight of the nine dividing cells in the anterior ectoderm of this animal are localized within the region of the presumptive brain (Fig. 6F, BR, shaded region). Clear visualization of spindles later than stage 3 is difficult due to an increase in tubulin and a decrease in cell size, resulting in a lack of spindle resolution throughout the anterior ectoderm. These data suggest that as cells are ingressing towards the end of stage 3, other cells are not simultaneously being internalized by oriented cell division.

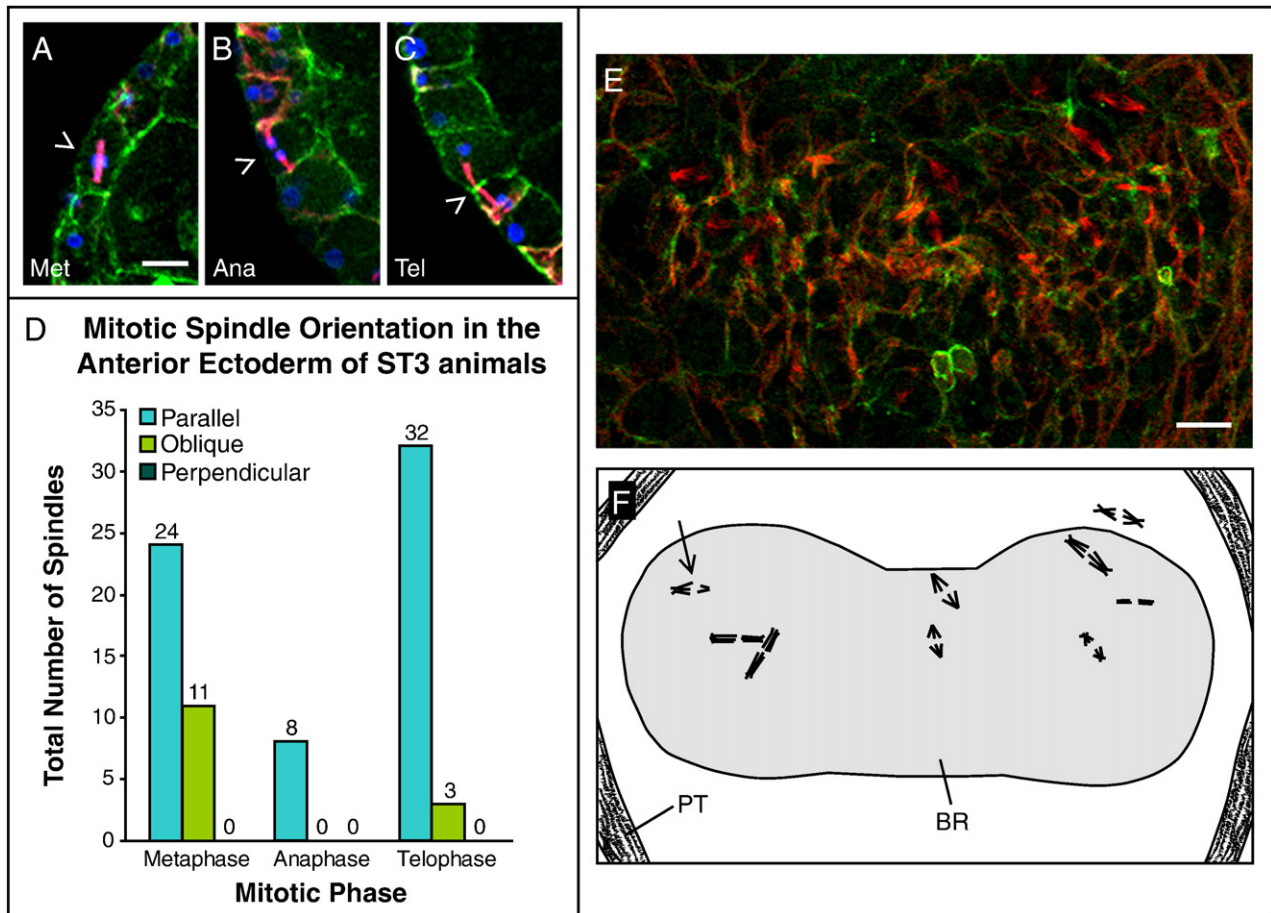


**Fig. 6.** Cleavage spindles in the anterior ectoderm are oriented parallel to the plane of the epithelium at stage 3. (A–C) Confocal micrographs of the anterior ectodermal thickening at stage 3 from a ventral view, anterior to the left, stained with anti-beta-tubulin (red, spindles), phalloidin (green, cell outlines), and anti-histone (blue, nuclei/chromatin). Mitotic metaphase (Met), anaphase (Ana) and telophase (Tel) spindles are denoted with arrowheads. (D) Graph depicting spindle orientation in the anterior ectodermal thickening from blastopore formation through the end of stage 3 ( $n = 26$  animals). (E) Stack of confocal images through the surface anterior ectoderm (depth of 2.5–4.5  $\mu\text{m}$ ) of a late stage 3 animal stained with anti-beta-tubulin (red) and phalloidin (green). (F) Diagram of spindles in E showing positions of the spindles relative to the presumptive brain (BR). Arrow indicates an oblique spindle. The position of the presumptive prototroch (PT) is drawn. E and F are anterior views, ventral down. The scale bars in A and E are 10  $\mu\text{m}$ . A–C are to the same scale.

#### Proliferation patterns in the anterior ectoderm

To address when and where *Capitella* sp. I brain NPCs are dividing, stages 3–9 animals were either incubated with the thymidine analog BrdU (incorporated during S-phase) or labeled with an anti-phosphohistone (phHist) antibody (labels mitotic prophase through beginning anaphase; Goto et al., 1999). Labeling with BrdU marks a larger percentage of cycling cells and their progeny than does the anti-phHist antibody, but the anti-phHist antibody provides precise positional information of dividing cells at the time of fixation. To minimize the possibility of cells incorporating BrdU and then ingressing, animals were incubated in BrdU for 30 min and immediately fixed. The location and number of BrdU<sup>+</sup> or phHist<sup>+</sup> cells are quantified in Figs. 7K–M (see also Fig. S3 and Tables S1–5).

During stage 3, when the anterior ectoderm is largely comprised of a monolayer of cells, BrdU is incorporated into cells with apically positioned nuclei (Figs. 7A, K, Figs. S4A, F). As the anterior ectoderm transitions from a monolayer to a multi-layered epithelium during stage 4, BrdU<sup>+</sup> nuclei are both apically (63%) and medially (33%) localized, but absent from a basal position (Figs. 7B, K, Figs. S4B, G). This trend continues through stage 5 (65% apical, 30% medial; Figs. 7C, K, Figs. S4C, H). By stage 6, most BrdU<sup>+</sup> nuclei are apically localized (early stage 6, 75% apical, 21% medial; Figs. 7D, K, Figs. S4D, I; late stage 6, 88% apical, 10% medial; Fig. 7K). The presence of internally positioned BrdU<sup>+</sup> cells in the yolkly endoderm, foregut (Fig. 7E, Figs. S4I, J), and occasionally brain (Fig. 7D, arrow) confirms that uptake of

BrdU or penetration of the anti-BrdU antibody does not prevent BrdU labeling in the brain. After stage 6, the total number of BrdU<sup>+</sup> nuclei declines, and most BrdU<sup>+</sup> cells in the head are localized to the epidermis (Figs. 7E, L, Figs. S4E, J). Thus, as the anterior ectoderm thickens and the brain forms, S-phase cells are largely limited to the surface ectodermal layer and not in internalized brain precursors.

To more precisely determine where cells are dividing within the anterior ectoderm, we analyzed phHist<sup>+</sup> nuclei in conjunction with phalloidin and anti-histone labeling. The number of phHist<sup>+</sup> cells with (surface) or without (sub-surface) an apical contact at stages 3–5 or in the epidermis (surface) or brain (sub-surface) at stages 6–9 was also quantified (Fig. 7M). From stages 3–5, most dividing anterior ectodermal cells maintain contact with the apical surface of the epithelial layer (Figs. 7F–H, arrowheads; M). Only a small subset does not have apical surface contacts (12/409 phHist<sup>+</sup> cells, 46 animals scored). We do not find any ingressing cells that are also phHist<sup>+</sup>, and, in general, dividing cells are not localized adjacent to ingressing cells. Additionally, of all the late stage 3 animals stained with anti-phHist, only one basal, squamous, phHist<sup>+</sup> cell was observed (not shown). At stages 6–8, once the brain is distinct from the overlying epidermis, the majority of dividing cells are localized to the epidermis (Figs. 7I, J, M). However, a small number of dividing cells are localized to the brain (12/255 phHist<sup>+</sup> cells, 53 animals scored). At stage 9, the total number of dividing cells is very low; we observed only 4 phHist<sup>+</sup> cells in the brain and 0 in the epidermis in 13 animals. In conclusion, these results suggest that the majority of anterior ectodermal cells divide on

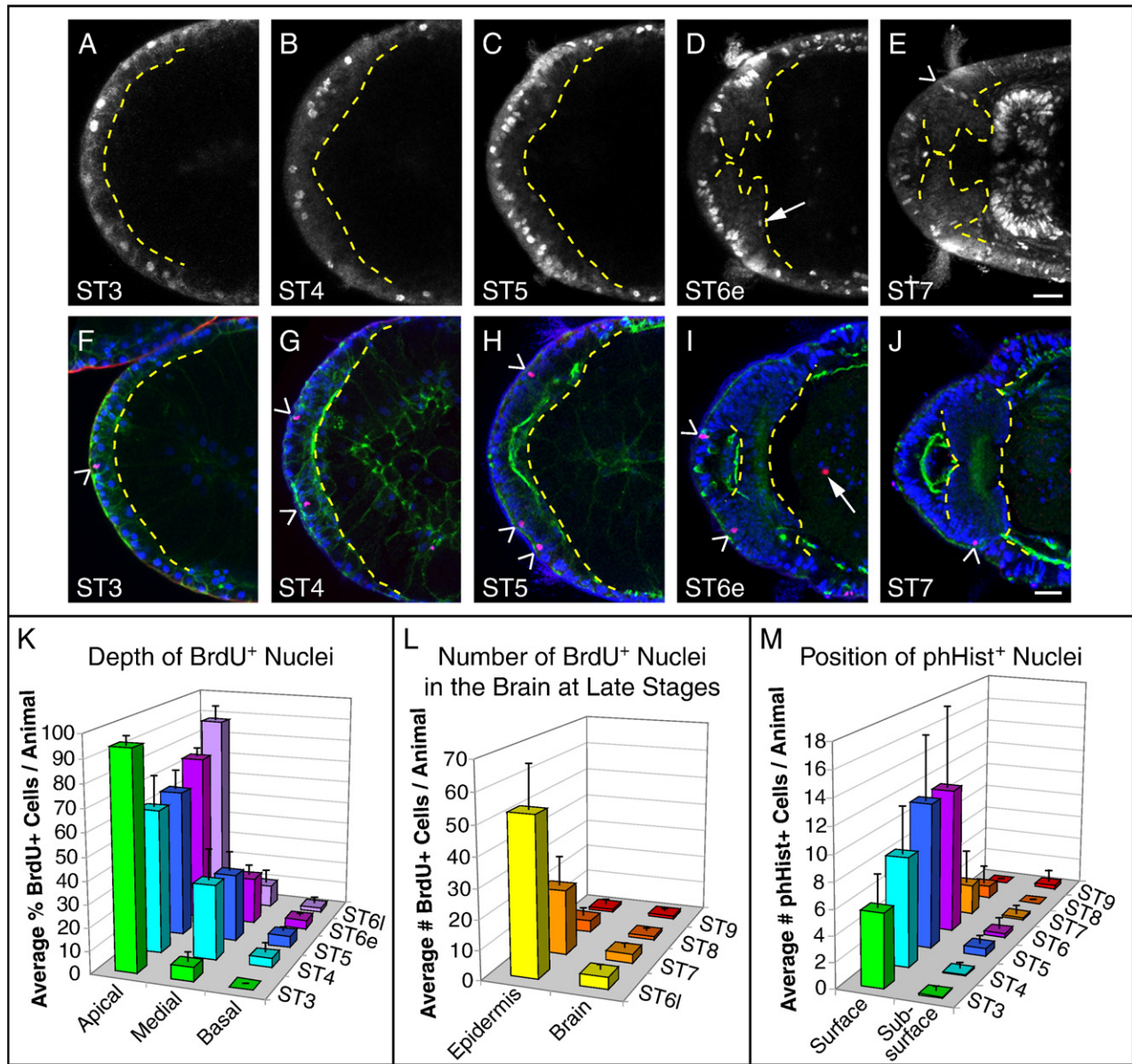


**Fig. 7.** Cycling cells are apically localized within the anterior ectoderm. (A–E) Single-channel, epifluorescent, confocal micrographs of anti-BrdU staining. Animals were incubated with BrdU for 30 min. A BrdU<sup>+</sup> cell in the brain is denoted with an arrow in D. A line of BrdU<sup>+</sup> cells localized to the lateral edge of the brain at stage 7 is denoted with an arrowhead in E. (F–J) Merged, epifluorescent, confocal micrographs of anti-phospho-histone (red), phalloidin (green) and anti-histone (blue) staining. Arrowheads in F–J denote apically localized phHist<sup>+</sup> nuclei in the anterior ectoderm. The arrow in I points to a phHist<sup>+</sup> cell in the foregut. (K) Graph depicting the average percent of BrdU<sup>+</sup> nuclei localized to the apical, medial or basal regions (see Fig. S3, Table S1) of the anterior ectodermal thickening at stages 3–6. (L) Graph depicting the average number of BrdU<sup>+</sup> nuclei in the head epidermis and brain at stages 6–9. (M) Graph depicting the average number of phHist<sup>+</sup> nuclei with (surface) or without (sub-surface) apical contacts at stages 3–5, and in the anterior epidermis (surface) or brain (sub-surface) at stages 6–9. Error bars in K–M represent the standard error of the mean. Images in A–J are ventral views, anterior to the left, and the stage of the animal is indicated in the lower left. A dashed line delineates the basal edge of the anterior ectodermal thickening in A–C and F–H. The dashed lines in D, E, I and J demarcate the anterior and posterior edges of the brain. The scale bars in E and J are 25  $\mu$ m. A–E and F–J are to the same scale as each other.

the apical surface of the epithelial layer. The small number of internal phHist<sup>+</sup> and BrdU<sup>+</sup> nuclei indicates that cells in the brain are also cycling, but likely at a much slower rate than on the surface.

#### *Capitella* sp. I *achaete-scute* homolog expression

To begin to characterize molecular mechanisms of NPC fate specification in *Capitella* sp. I, we scanned the *Capitella* sp. I genome and EST libraries and identified five *achaete-scute* family members. Alignment of the predicted protein sequences for these five genes with other Asc family members shows a highly conserved bHLH domain (Fig. S5A). Bayesian and neighbor-joining analyses place all five within the asc family (Fig. S5B); two group with other ASCa subgroup genes

(*Capl-ash1*, *Capl-ash2*), one with ASCb subgroup genes (*Capl-ash3*) and two with ASC-like subgroup genes (*Capl-ash4*, *Capl-ash5*). ASCa subgroup genes have a conserved proneural function or are expressed in a manner consistent with a proneural function in other animals (Bertrand et al., 2002; Stollewerk and Simpson, 2005); therefore, we examined expression of these two homologs in *Capitella* sp. I. Both genes are expressed during brain development, but the *Capl-ash1* expression pattern is consistent with a possible proneural function. *Capl-ash2* is more broadly expressed in all three germ layers, including in the developing brain. Consequently, we focused on describing the *Capl-ash1* expression pattern during brain development.

*Capl-ash1* is initially expressed prior to NPC ingress during mid-epiboly in a small patch of ectodermal cells on the animal side of the

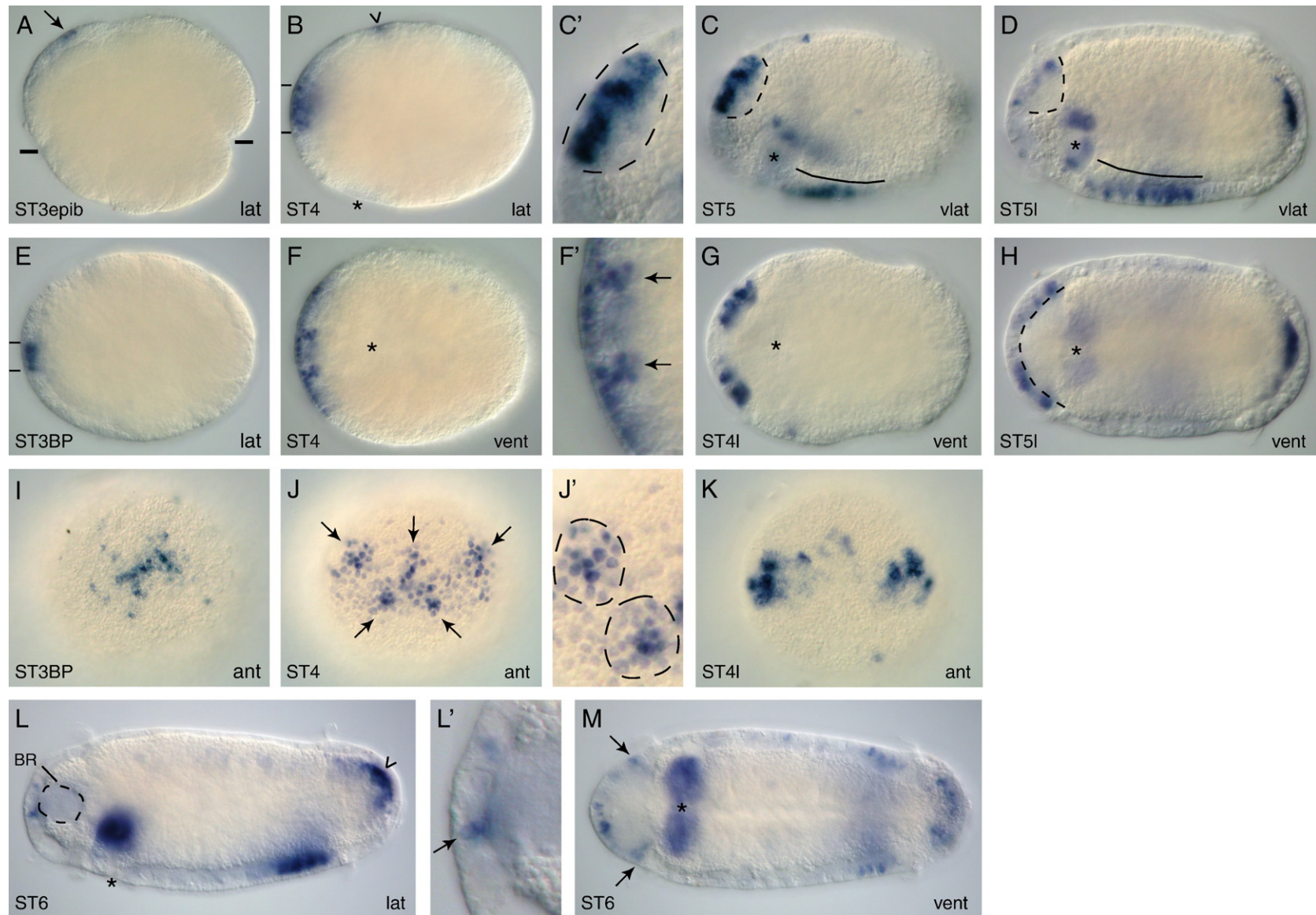


**Fig. 8.** *Capl-ash1* is expressed in the anterior ectodermal thickening prior to and during NPC ingress. (A–M) *Capl-ash1* transcript was detected in stage 3–6 animals by in situ hybridization. Arrow in A points to early *Capl-ash1* expression in a few ectodermal cells. The epibolizing front of the gastrula is marked with two lines. An arrowhead in B marks a patch of dorsal, *Capl-ash1*<sup>+</sup> cells. Two lines in B and E indicate the medial patch of anterior ectodermal *Capl-ash1* expression. A dashed line in C, C' and D denotes one side of the anterior ectodermal thickening. Arrows in F' indicate 'fingers' of more basal *Capl-ash1* expression. A dashed line in H marks a possible boundary between presumptive epidermis and brain. Five patches of prominent *Capl-ash1* expression are indicated with arrows in J, two of which are outlined with dashed circles in J'. A dashed circle in L outlines the brain (BR), and an arrowhead indicates *Capl-ash1* expression in possible visceral mesodermal precursors. An arrow in L' points to a single, *Capl-ash1*<sup>+</sup> epidermal cell. Arrows in M point to sub-surface, *Capl-ash1*<sup>+</sup> cells positioned at the lateral edges of the brain. In each panel, the stage of the animal is indicated in the lower left, and the view is indicated in the lower right (lat, lateral; vlat, ventrolateral; vent, ventral; ant, anterior). In all lateral and ventrolateral views, anterior is to the left and ventral down; in all ventral views, anterior is to the left; and in all anterior views ventral is down. Panels C', F', J' and L' are higher magnification, cropped images of C, F, J and L, respectively. J' is a higher magnification image of the left side of J. An asterisk marks the position of the mouth, and in ventrolateral views (C, D) a line marks the position of the ventral midline.

embryo (Fig. 8A, arrow). This region of ectoderm is slightly thicker than the surrounding ectoderm. We think that this expression domain corresponds to the future region of ectoderm from which brain NPCs will ingress. Several hours later (late-epiboly), a region of thicker ectoderm is more vegetally positioned and expresses *Capl-ash1* (not shown). Furthermore, Dil labeling of this ectodermal region at late-epiboly results in Dil<sup>+</sup> brain polyclones a few days later (not shown). By the end of gastrulation, *Capl-ash1* is expressed in a larger patch of medial, anterior ectodermal cells (Figs. 8E, I), where presumptive brain NPCs are ingressing. From stage 3 to stage 4, this expression domain expands slightly dorsoventrally (compare dashes in Fig. 8B with those in E) and laterally (compare Fig. 8J with I), resulting in five patches of prominent surface expression (Fig. 8J, arrows; J', dashed circles) positioned within a broader expression domain. Each of the five patches of strong expression corresponds to ~10–20 cells and is reproducibly observed across similarly staged animals. Within each of the five patches, *Capl-ash1* is expressed at an even higher level in ~1–3 cells. In addition to the surface ectodermal expression of *Capl-ash1* during stage 4, clusters (~3–5) of deeper cells in the region of the anterior ectodermal thickening also express *Capl-ash1* (Figs. 8F; F', arrows).

From the end of stage 4 into early stage 5, *Capl-ash1* expression decreases medially in the anterior ectoderm and is present in lateral patches in the region of the forming brain (Figs. 8C, G, K; compare K with J). Early during stage 5, *Capl-ash1* is restricted to the apical half of the anterior ectodermal thickening (Figs. 8C, C'), and by late stage 5 and early stage 6, *Capl-ash1* is expressed in the apical third of the anterior ectodermal thickening, likely in the epidermis (Figs. 8D, H). These lateral regions of *Capl-ash1* expression may correspond to regions of continued cell ingression. As the brain becomes morphologically distinct from the overlying epidermis (late stage 6), *Capl-ash1* is largely absent from the brain (Fig. 8L, BR) but is expressed in isolated, surface epidermal cells that may correspond to presumptive sensory cells (Fig. 8L', arrow). At these stages, *Capl-ash1* is also expressed in sub-surface cells at the lateral edges of the developing brain (Fig. 8M, arrows). These *Capl-ash1*<sup>+</sup> cells positionally coincide with BrdU<sup>+</sup> cells at stages 6–7 (Fig. 7E, arrowhead). By stage 8, *Capl-ash1* is not expressed in the head. In summary, the expression patterns we observe in the anterior ectoderm are compatible with a proneural function for *Capl-ash1* in fate specification and internalization of brain NPCs in *Capitella* sp. I.

In addition to the anterior ectoderm, *Capl-ash1* is expressed in a number of other distinct regions. From stages 5 to 8, *Capl-ash1* transcript is detected in patches in the ventrolateral ectoderm (e.g., Fig. 8D) and in single cells in the body ectoderm (presumably in ventral nerve cord precursors and forming sensory cells, respectively). *Capl-ash1* is also expressed in a cluster of ectodermal cells just posterior to the prototroch during stages 3–5 (e.g., Fig. 8B, arrowhead), in a small cluster of posterior ectodermal cells from stages 3 to 4 where the anus will form (not shown), and in the developing foregut from stages 5 to 8 (Figs. 8D, L, M). *Capl-ash1* is also expressed in presumptive mesodermal stem cells during stage 3 (not shown) and in a cluster of sub-surface posterior cells starting at stage 5 (Figs. 8D, H). This sub-surface, posterior expression domain expands anteriorly from stages 6 to 8. These *Capl-ash1*<sup>+</sup> cells appear migratory in shape, are located between the body wall muscle and endoderm, and may be visceral mesoderm precursors (e.g., Fig. 8L, arrowhead). By stage 9, *Capl-ash1* transcript is not detectable by *in situ* hybridization.

#### *Capitella* sp. I Notch and Delta homolog expression

To determine whether Notch signaling could be involved in early brain neurogenesis, we characterized *Capl-Notch* and *Capl-Delta* expression in the anterior ectoderm of stages 3–4 animals. *Capl-Notch* and *Capl-Delta* expression patterns have previously been

reported, but with emphasis on expression in the trunk rather than in the anterior ectoderm (Thamm and Seaver, 2008). In addition to other domains, *Capl-Delta* transcript is detected early during gastrulation in a small patch of ectodermal cells on the animal side of the embryo (not shown). By the end of gastrulation, *Capl-Delta* is highly expressed in a medial cluster of cells in the anterior ectoderm with lower levels of expression in surrounding cells (Figs. S6A, B, arrows). This expression domain expands laterally by stage 4 and appears to be both on the surface and deeper within the anterior ectoderm (Figs. S6C, D, arrows). *Capl-Delta* is expressed with varying levels of intensity in the anterior ectoderm throughout stages 3 and 4, and the regions of highest *Capl-Delta* expression roughly correspond to the patches of high *Capl-ash1* expression at similar stages (compare Fig. S6A with Fig. 8I and Fig. S6C with Fig. 8J). *Capl-Notch* is not detected in the anterior ectoderm during stage 3, although transcript is detected elsewhere in the embryo (not shown). By early stage 4, *Capl-Notch* is expressed in a few basally positioned cells within the medial, anterior ectoderm (Figs. S6E, F, arrows). The expression pattern of *Capl-Notch* expands laterally during stage 4, and transcript is detected both on the surface and basally (Fig. S6G, H). *Capl-Notch* surface expression is heterogeneous at stage 4 (Fig. S6G), although distinct from the pattern observed for *Capl-ash1* and *Capl-Delta*. Overall, the expression patterns of *Capl-Delta* and *Capl-Notch* are consistent with a possible role during brain neurogenesis. Furthermore, the pattern of *Capl-Delta* closely resembles the pattern of *Capl-ash1* from early gastrulation through late stage 4.

#### *Capitella* sp. I *elav* homolog expression

The *elav/hu* family of genes encode RNA binding proteins expressed in post-mitotic neurons in a wide range of animals (Berger et al., 2007; Pascale et al., 2008; Robinow and White, 1991; Wakamatsu and Weston, 1997). Because *elav/hu* genes are one of the earliest markers for neural cells as they begin to differentiate and exit the cell cycle, we screened for *Capitella* sp. I homologs. A thorough search of the *Capitella* sp. I genome and EST libraries yielded two putative *elav/hu* homologs, *Capl-elav1* and *Capl-elav2*. *Elav/Hu* family members are defined by two closely spaced RNA recognition motifs (RRM1 and RRM2) followed by a hinge region and then a third RNA recognition motif (RRM3) (Birney et al., 1993; Samson, 2008). Alignment of *Capitella* sp. I *Elav* predicted protein sequences with other *Elav/Hu* homologs shows this RRM domain structure (Fig. S7A). Bayesian and neighbor-joining analyses place both putative *Capitella* sp. I *elav* genes within the *elav/hu* family. *Capl-elav1* groups within a clade that includes neural *elav/hu* family members (Fig. S7B, turquoise). *Capl-elav2* groups separately with two other molluscan *elav/hu* family members (Fig. S7B, green). Based on our searches of arthropod, deuterostome and lophotrochozoan genomes and based on a recent gene orthology analysis of *elav* genes in arthropods and humans (Samson, 2008), *Capl-elav2* may belong to a lophotrochozoan-specific *elav/hu* clade (Fig. S7B, green). Both *Capl-elav1* and *Capl-elav2* were cloned and their expression patterns characterized during early *Capitella* sp. I brain development. Because *Capl-elav1* shows the most specific neural pattern, we describe its expression here. *Capl-elav2* is primarily expressed in mesoderm precursors and to a lesser extent in the brain (not shown).

*Capl-elav1* transcript is first detected in a few basally localized cells in the anterior ectodermal thickening during late stage 3, just after the mouth has formed (arrows in Figs. 9A, E; I). At this stage only a few cells have apically detached from the epithelium (Fig. 5L, turquoise cells, filled arrowhead). A few hours later, *Capl-elav1* expression expands to several cells in the anterior ectoderm (compare Fig. 9I with J). This *Capl-elav1* expression domain continues to expand slightly through stage 4, and remains basally localized within the anterior ectodermal thickening (Figs. 9B, F, F'). The expansion in *Capl-elav1* expression from late stage 3 to early stage 4 corresponds with an

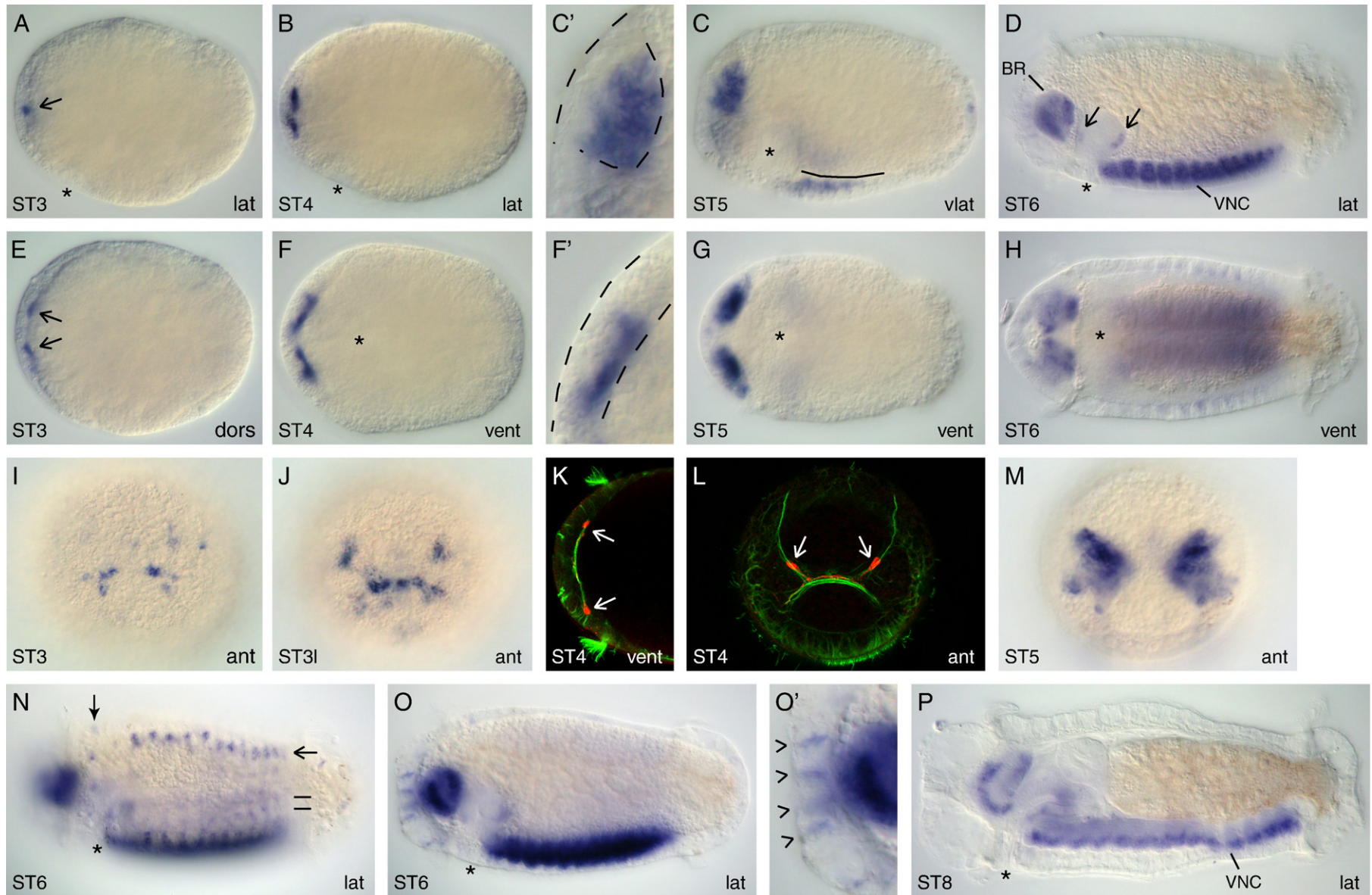


**Fig. 9.** *Capl-elav1* is expressed in the developing CNS. (A–J, M–P) *Capl-elav1* was detected in stage 3–8 animals by in situ hybridization. Arrows in A and E point to the first *Capl-elav1*<sup>+</sup> cells in the anterior ectodermal thickening. Dashed lines in C' outline one side of the anterior ectodermal thickening. A line in C marks the ventral midline. Arrows in D point to *Capl-elav1* expression in the developing foregut. Panels C, F, and O' are higher magnification, images of C, F and O, respectively. Arrows in N denote rows of *Capl-elav1*<sup>+</sup> cells in the plane of focus, and lines denote rows out of the plane of focus. Arrowheads in O' indicate single *Capl-elav1*<sup>+</sup> epidermal cells. (K, L) Merged, epifluorescent confocal images of stage 4 animals stained with anti-acetylated tubulin (green, axon tracts) and anti-Serotonin (red). Arrows in K and L indicate the soma of serotonergic neurons in the brain. In each panel, the stage of the animal is indicated in the lower left, and the view is indicated in the lower right (lat, lateral; vlat, ventrolateral; vent, ventral; ant, anterior). In all lateral and ventrolateral views, anterior is to the left and ventral down; in all ventral views, anterior is to the left; and in all anterior views ventral is down. An asterisk marks the position of the mouth. BR, brain; VNC, ventral nerve cord.

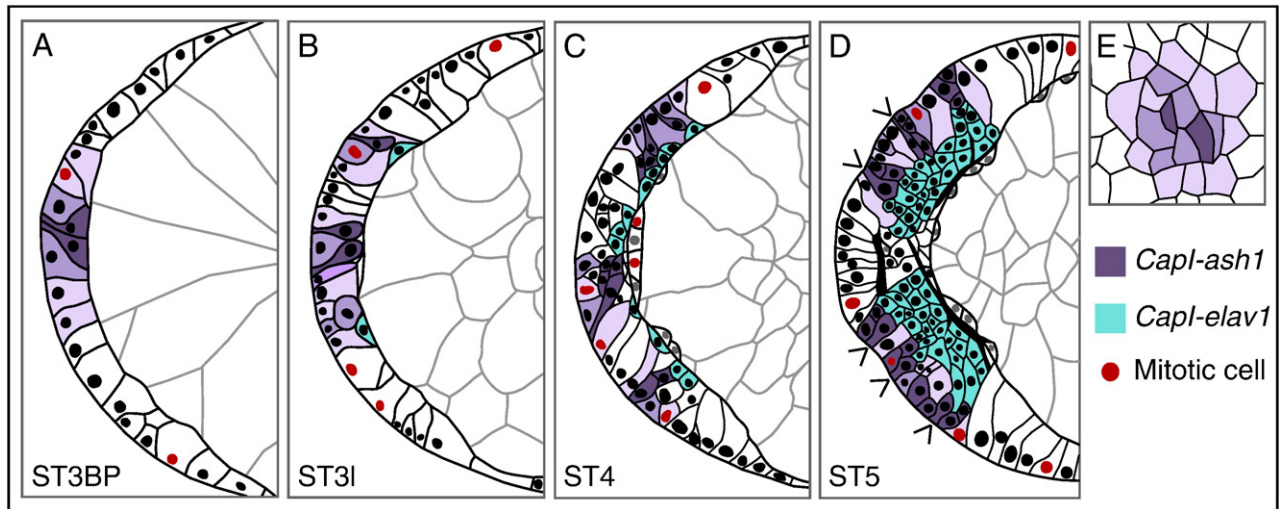


**Fig. 10.** Model of *Capitella sp. I* brain development. (A–D) Diagrams from stages 3 to 5 depicting the transition of the anterior ectoderm from a simple, cuboidal epithelium to a stratified epithelium during early brain development. *Capl-ash1* expression is indicated by varying shades of purple, with dark purple signifying high levels of expression. *Capl-elav1* expression is shown in turquoise, and mitotic nuclei are indicated in red. Cell outlines and nuclei in A, B and C were traced from the animals shown in Figs. 5C, K and S, respectively, but from a wider range of confocal slices. Cell outlines and nuclei in D were traced based on confocal images of a stage 5 animal stained with phalloidin and anti-histone. Arrowheads in D indicate bottle cells. In A–D, the stages are represented in the lower left. A–D are ventral views, anterior to the left. (E) A diagram of a patch of *Capl-ash1*<sup>+</sup> cells from an anterior view. Cell outlines were traced based on confocal images of a late stage 3 animal stained with phalloidin and anti-histone.

increase in the number of internalized cells in similarly staged animals (Fig. 5T). At stage 5, *Capl-elav1* is basally expressed within the anterior ectodermal thickening, which is the presumptive brain (Figs. 9C, C', G, M). *Capl-elav1* shows continued expression in the brain from stages 6 to 9 (Figs. 9D, BR; H, O, P) and after metamorphosis in juveniles (not shown).

The localization of *Capl-elav1* in the developing brain contrasts with that of *Capl-ash1* and the positions of dividing cells at similar stages. *Capl-elav1* is basally localized while *Capl-ash1* and dividing cells are predominantly apically localized (compare Fig. 9F' with Fig. 8F' and Fig. 9C' with Fig. 8C'). The first apparent axon tracts in *Capitella sp. I* are visible in the brain by late stage 4 (Figs. 9K and L, green). The first two serotonergic neurons appear soon thereafter, and their soma are basally positioned at the lateral edges of the anterior ectodermal thickening (Figs. 9K and L, arrows). The timing of expression and position of *Capl-elav1*<sup>+</sup> cells relative to dividing cells and differentiated neurons suggests that *Capl-elav1* is expressed in neural cells just prior to and throughout their differentiation (compare Figs. 9F with K and J with L).

In addition to expression in the brain, *Capl-elav1* transcript is also detected in other regions of the nervous system. Ventral nerve cord expression is observed from stage 5 through metamorphosis (see Figs. 9D, P, VNC). During stages 6–7, single and small clusters of *Capl-elav1*<sup>+</sup> ectodermal cells are present in the head, body and pygidium, presumably the developing peripheral nervous system. Single ectodermal cells expressing *Capl-elav1* in the head are shown in Figs. 9O and O' (arrowheads). A circumferential row of *Capl-elav1*<sup>+</sup> cells is positioned just posterior to the prototroch (Fig. 9N, closed arrow). In the body, there are at least six rows (three on each side of the animal) consisting of small clusters of segmentally-iterated *Capl-elav1*<sup>+</sup> ectodermal cells (e.g., Fig. 9N, open arrow). *Capl-elav1* is also expressed from late stage 4 through stage 5 in two small, posterior patches of ectoderm (not shown). From stage 6 through metamorphosis, *Capl-elav1* is expressed in the developing foregut in a bilateral pair of cell clusters (4 total), one each associated with anterior and posterior edges of the foregut (Fig. 9D, arrows). These expression domains may correspond to the developing enteric nervous system. Overall, *Capl-elav1* is broadly expressed in the developing nervous system, including in brain NPCs as they become post-mitotic.

## Discussion

### Model of early brain neurogenesis in *Capitella sp. I*

Our combined approach has led us to propose a model (Fig. 10) in which multiple cells expressing the highest levels of *Capl-ash1* ingress as single cells from each proneural domain in the anterior ectoderm (Fig. 10E). This results in localized regions of ingression during stages 3 and 4 (Figs. 10A–C). By stage 5, brain NPC internalization is reduced, and obvious bottle cells are not observed. However, cells with slightly constricted apical membranes are present (Fig. 10D, arrowheads), indicating that at stage 5 NPCs may continue ingressing from lateral regions of high *Capl-ash1* expression (Fig. 10D). After ingression, NPCs have a limited proliferative potential and express *Capl-elav1* and the neural differentiation marker *synaptotagmin* (N.P.M., unpublished data). Their final neural fate may not yet be determined, and at stages 4 and 5, homologs of neural 'patterning' genes (e.g., *gsx/ind* (Froebius and Seaver, 2006b), *homeobrain* (Froebius and Seaver, 2006a), *pax6*, *runt*, and *coe*, Seaver lab, unpublished data) are expressed in subsets of basally localized cells within the anterior ectodermal thickening. This is consistent with the possibility that neural subtype patterning may occur after internalization. As a result of brain NPC ingression, the anterior ectoderm transitions from a simple epithelium at stage 3 to a stratified epithelium consisting of an outer epidermal and an inner neural layer by stage 5. These layers eventually form the epidermis and brain.

### Comparisons of *Capitella sp. I* neurogenesis with other bilaterians

#### Cellular mechanisms: segregating NPCs from the ectoderm

Cellular mechanisms of NPC internalization are fairly distinct between vertebrates and insects, with the invagination of a sheet of cells versus ingression of single cells, respectively. In non-insect arthropods, the cellular mechanisms of internalization are somewhat intermediate, involving ingression of groups of NPCs initially and overgrowth of a sheet of neuroectoderm by epidermis secondarily (Dove and Stollewerk, 2003; Kadner and Stollewerk, 2004; Stollewerk et al., 2001). Detailed, cellular-resolution data demonstrating ingression as a cellular mechanism of NPC internalization were previously confined to Ecdysozoa, but with the addition of our data from *Capitella*

sp. I, ingression of NPCs is now shared by at least one annelid. In the mollusk *A. californica*, NPCs migrate across the animal to form the ganglia. Although bottle cells were not explicitly described (Jacob, 1984), bottle-cell formation often precedes internalization and migration (Shook and Keller, 2003), and we suggest that neurogenesis in this mollusk may also involve ingression. The evolutionary significance of ingression as a shared cellular mechanism for internalizing NPCs awaits data from other lophotrochozoans and earlier branching arthropods.

Our initial characterization of early neurogenesis in *Capitella* sp. I focuses on brain development. In some animals where both brain and trunk neurogenesis have been studied, the cellular mechanisms of neurogenesis are often similar. There is evidence from spiders and myriapods that both brain and ventral nerve cord NPCs are internalized by ingression of groups of cells (Dove and Stollewerk, 2003; Kadner and Stollewerk, 2004; Stollewerk et al., 2001). This is also the case in the mollusk *A. californica* in which brain and trunk ganglia develop by the same cellular mechanisms (Jacob, 1984). Conversely, in *D. melanogaster*, the cellular mechanisms of brain and trunk neurogenesis are distinct. Unlike ventral nerve cord neuroblasts, *D. melanogaster* brain neuroblasts segregate continuously rather than in discrete waves. Furthermore, brain neuroblasts in close proximity to one another can ingress (Hartenstein and Campos-Ortega, 1984; Urbach et al., 2003), which is reminiscent of brain neurogenesis in *Capitella* sp. I.

The embryonic origins of the brain and ventral nerve cord are quite distinct in *Capitella* sp. I, as well as in other animals that develop by spiral cleavage (spiralian). The brain is generated from descendants of first quartet micromeres while the ventral nerve cord is generated from descendants of the 2d micromere (Ackermann et al., 2005; Henry, 1999; Nielsen, 2004; N.P.M., unpublished data). In *Capitella* sp. I, this means that the brain develops from anterior, unsegmented ectoderm, while the ventral nerve cord develops from segmented, trunk ectoderm. Thus, we think that there are likely differences between brain and ventral nerve cord development in *Capitella* sp. I.

#### Limiting the number of ingressing cells through *Asc* and *Notch* activity

In arthropods, species-specific differences in ingression appear to be primarily in the number of cells that ingress from a single, proneural expression domain. This raises the question of how the number of ingressing cells is determined and whether *asc* homologs control this process. In some regions of the *D. melanogaster* head ectoderm, single neighboring neuroblasts ingress from the same domain of proneural gene (*l'sc*) expression, and *l'sc* continues to be expressed in surrounding cells after a neuroblast segregates (Urbach et al., 2003; Younossi-Hartenstein et al., 1996). This is distinct from the *D. melanogaster* ventral nerve cord in which only one neuroblast forms from each proneural domain, and *l'sc* expression is downregulated in cells surrounding the neuroblast after it ingresses (Cabrera et al., 1987; Martin-Bermudo et al., 1991; Skeath and Thor, 2003). Furthermore, the expression domain of *l'sc* in the head ectoderm is much broader than in the ventral nerve cord (Urbach et al., 2003; Younossi-Hartenstein et al., 1996). Urbach et al. (2003) suggest that the lack of *l'sc* downregulation may result from decreased lateral inhibition via *Notch* signaling in the procephalic ectoderm. In the spider *C. salei*, almost all cells in a proneural cluster ingress and become neural (Stollewerk et al., 2001). Stollewerk suggests that in the spider neuroectoderm, *CsASH1* is initially expressed in larger clusters of cells than in the *D. melanogaster* neuroectoderm. High levels of proneural gene expression in a larger group of cells results in higher levels of *Delta* expression in all cells of the group, making them insensitive to *Notch* signaling, since a high ratio of *Delta* to *Notch* levels within a cell may block reception of a *Notch* signal (Doherty et al., 1996; Stollewerk, 2002). These results from arthropods suggest that the number of NPCs arising from a region of ectoderm is controlled both by the number of

adjacent cells with high levels of proneural gene expression, and the ability of a cell to receive a *Notch* signal.

In the *Capitella* sp. I head region at stage 4, the highest levels of *Capl-ash1* transcript are detected in ~1–3 neighboring cells with intermediate levels of transcript in several surrounding cells, which together form one proneural patch. At the same stage, *Capl-Delta* and *Capl-Notch* are heterogeneously expressed throughout the anterior ectoderm. *Capl-Delta* expression closely resembles the pattern of *Capl-ash1* from stages 3 to 4, which is consistent with a possible function for *CaplAsh1* in upregulating *Capl-Delta* transcription as has been shown in other animals (Akai et al., 2005; Bertrand et al., 2002; Kunisch et al., 1994). High levels of *Capl-ash1* expression in more than one neighboring cell in a proneural patch and potentially high levels of *Capl-Delta* in the same *Capl-ash1*<sup>+</sup> cells may inhibit the ability of these cells to receive a *Notch* signal, thus allowing more than one NPC to ingress from the same proneural patch in *Capitella* sp. I.

#### *Asc* function in neural fate specification

In addition to influencing the number of cells that ingress from a proneural domain, *Asc* homologs also function across taxa in NPC fate specification. The type of fate decision *Asc* homologs promote varies in different contexts and does not seem to be clade-specific. In *D. melanogaster*, *Asc* homologs specify neural fate at the expense of epidermal fate (Doe and Goodman, 1985b; Skeath and Thor, 2003). In contrast, recent data from spiders and myriapods suggests that proneural genes select NPCs from a field of cells that may already be committed to a neural fate (Chipman and Stollewerk, 2006; Dove and Stollewerk, 2003; Stollewerk, 2002). Similarly, in many vertebrates, proneural genes act in cells that are already committed to a neural fate, likely promoting neural differentiation at the expense of gliogenesis (Bertrand et al., 2002; Nieto et al., 2001; Tomita et al., 2000; Turner and Weintraub, 1994). During *Capitella* sp. I brain neurogenesis, at least one proneural gene (*Capl-ash1*) is expressed in a pattern consistent with a function in selecting neural cells. It seems unlikely that *Capl-ash1* acts to select NPCs from a field of cells already committed to a neural fate, since our *Dil* labeling experiments did not produce neural-only polyclones (Table 1, second column). Thus, in *Capitella* sp. I, neural and epidermal precursors reside in close proximity to one another in the anterior ectoderm. Furthermore, the same precursor may produce both neural and epidermal daughters. In this respect, *Capitella* sp. I brain neurogenesis is more similar to *D. melanogaster* neurogenesis, in which neural and epidermal precursors reside next to each other.

Another aspect of *Asc* function that varies across species is the timing of NPC fate specification relative to reduction in proliferative potential. In *D. melanogaster*, individual neuroblasts are fate specified by *Asc* prior to the cell divisions that produce neurons and glial cells (Pearson and Doe, 2004; Skeath, 1999; Skeath and Thor, 2003). In contrast, in *C. salei*, NPCs largely do not divide after ingression (Stollewerk et al., 2001). Thus, a spider *asc* homolog may select NPCs after they have already divided or may promote neural differentiation. This would be similar to vertebrates, in which high levels of proneural gene expression promote cell cycle arrest and eventual neural differentiation (Bertrand et al., 2002; Farah et al., 2000).

In *Capitella* sp. I, we propose that *Capl-ash1* either specifies NPCs after they have divided or promotes neural differentiation, similar to the function in spiders and vertebrates. In the annelid *P. dumerilii*, the proneural genes *Pdu-ash* and *Pdu-ngn* are expressed apically within the ventral neuroectoderm while neural differentiation markers are expressed more basally (Simionato et al., 2008). At the same stage, *BrdU*<sup>+</sup> cells are restricted to the apical surface of the ventral neuroectoderm (Denes et al., 2007). These results seem similar to brain neurogenesis in *Capitella* sp. I, although the cellular details of early neurogenesis in *P. dumerilii* have not been reported to our knowledge. Furthermore, Simionato et al. interpret *Pdu-ash* expression as being consistent with a role in specifying neural subtype

identity rather than in specifying NPCs as appears to be the case in *Capitella* sp. I (Simionato et al., 2008). Another interesting difference is that in *Capitella* sp. I, clusters of basal cells express *Cap1-ash1*, whereas in *P. dumerilii* they do not. *Cap1-ash1* expression in basally localized cells is similar to that observed in insects, spiders and myriapods, which continue to express *asc* homologs after NPC ingress (Cabrera et al., 1987; Dove and Stollewerk, 2003; Skeath and Carroll, 1992; Stollewerk et al., 2001; Urbach et al., 2003). These differences between *P. dumerilii* and *Capitella* sp. I neurogenesis may either reflect differences between the ventral nerve cord and brain or species-specific differences.

## Conclusions

As a result of this study, we have developed a detailed model of brain neurogenesis in the annelid *Capitella* sp. I. Interestingly, *Capitella* sp. I neurogenesis shares many characteristics with arthropod neurogenesis, although some aspects appear more similar to insects while others are more similar to spiders and myriapods. Given the large phylogenetic separation between annelids and arthropods, it will be necessary to characterize neurogenesis in a wider range of taxa, including additional lophotrochozoans, to determine if these similarities are evolutionarily significant. Additional studies in *Capitella* sp. I will facilitate more in depth comparisons within the same animal and with other taxa.

## Acknowledgments

We thank C.R. Magie, P.N. Lee and K. Pang for comments on this manuscript. The *Capitella* sp. I genome and EST sequence data were produced by the US Department of Energy Joint Genome Institute (<http://www.jgi.gov>). This work was supported by the Wagner Blindness Prevention Fund of the Hawaii Community Foundation and the National Science Foundation (IOB05-44869) to E.C.S.

## Appendix A. Supplementary data

Supplementary data associated with this article can be found, in the online version, at doi:10.1016/j.ydbio.2009.06.017.

## References

Ackermann, C., Dorresteyn, A., Fischer, A., 2005. Clonal domains in postlarval *Platynereis dumerilii* (Annelida: Polychaeta). *J. Morphol.* 266, 258–280.

Akai, J., Halley, P.A., Storey, K.G., 2005. FGF-dependent Notch signaling maintains the spinal cord stem zone. *Genes Dev.* 19, 2877–2887.

Berger, C., Renner, S., Luer, K., Technau, G.M., 2007. The commonly used marker ELAV is transiently expressed in neuroblasts and glial cells in the *Drosophila* embryonic CNS. *Dev. Dyn.* 236, 3562–3568.

Bertrand, N., Castro, D.S., Guillemot, F., 2002. Proneural genes and the specification of neural cell types. *Nat. Rev. Neurosci.* 3, 517–530.

Birgbauer, E., Fraser, S.E., 1994. Violation of cell lineage restriction compartments in the chick hindbrain. *Development* 120, 1347–1356.

Birney, E., Kumar, S., Krainer, A.R., 1993. Analysis of the RNA-recognition motif and RS and RGG domains: conservation in metazoan pre-mRNA splicing factors. *Nucleic Acids Res.* 21, 5803–5816.

Cabrera, C.V., Martinez-Arias, A., Bate, M., 1987. The expression of three members of the achaete–scute gene complex correlates with neuroblast segregation in *Drosophila*. *Cell* 50, 425–433.

Casasosa, S., Fode, C., Guillemot, F., 1999. Mash1 regulates neurogenesis in the ventral telencephalon. *Development* 126, 525–534.

Chipman, A.D., Stollewerk, A., 2006. Specification of neural precursor identity in the geophilomorph centipede *Strigamia maritima*. *Dev. Biol.* 290, 337–350.

Chitnis, A., Kintner, C., 1996. Sensitivity of proneural genes to lateral inhibition affects the pattern of primary neurons in *Xenopus* embryos. *Development* 122, 2295–2301.

Denes, A.S., Jekely, G., Steinmetz, P.R., Raible, F., Snyman, H., Prud'homme, B., Ferrier, D.E., Balavoine, G., Arendt, D., 2007. Molecular architecture of annelid nerve cord supports common origin of nervous system centralization in bilateria. *Cell* 129, 277–288.

Diez del Corral, R., Breitkreuz, D.N., Storey, K.G., 2002. Onset of neuronal differentiation is regulated by paraxial mesoderm and requires attenuation of FGF signalling. *Development* 129, 1681–1691.

Doe, C.Q., 1992. Molecular markers for identified neuroblasts and ganglion mother cells in the *Drosophila* central nervous system. *Development* 116, 855–863.

Doe, C.Q., Goodman, C.S., 1985a. Early events in insect neurogenesis. I. Development and segmental differences in the pattern of neuronal precursor cells. *Dev. Biol.* 111, 193–205.

Doe, C.Q., Goodman, C.S., 1985b. Early events in insect neurogenesis. II. The role of cell interactions and cell lineage in the determination of neuronal precursor cells. *Dev. Biol.* 111, 206–219.

Doe, C.Q., Fuerstenberg, S., Peng, C.Y., 1998. Neural stem cells: from fly to vertebrates. *J. Neurobiol.* 36, 111–127.

Doherty, D., Feger, G., Younger-Shepherd, S., Jan, L.Y., Jan, Y.N., 1996. Delta is a ventral to dorsal signal complementary to Serrate, another Notch ligand, in *Drosophila* wing formation. *Genes Dev.* 10, 421–434.

Dove, H., Stollewerk, A., 2003. Comparative analysis of neurogenesis in the myriapod *Glomeris marginata* (Diplopoda) suggests more similarities to chelicerates than to insects. *Development* 130, 2161–2171.

Farah, M.H., Olson, J.M., Sucic, H.B., Hume, R.L., Tapscott, S.J., Turner, D.L., 2000. Generation of neurons by transient expression of neural bHLH proteins in mammalian cells. *Development* 127, 693–702.

Frobius, A.C., Seaver, E.C., 2006a. *Capitella* sp. I homeobrain-like, the first lophotrochozoan member of a novel paired-like homeobox gene family. *Gene Expr. Patterns* 6, 985–991.

Frobius, A.C., Seaver, E.C., 2006b. ParaHox gene expression in the polychaete annelid *Capitella* sp. I. *Dev. Genes Evol.* 216, 81–88.

Goto, H., Tomono, Y., Ajiro, K., Kosako, H., Fujita, M., Sakurai, M., Okawa, K., Iwamatsu, A., Okigaki, T., Takahashi, T., Inagaki, M., 1999. Identification of a novel phosphorylation site on histone H3 coupled with mitotic chromosome condensation. *J. Biol. Chem.* 274, 25543–25549.

Hammerle, B., Tejedor, F.J., 2007. A novel function of DELTA-NOTCH signalling mediates the transition from proliferation to neurogenesis in neural progenitor cells. *PLoS ONE* 2, e1169.

Hartenstein, V., Campos-Ortega, J.A., 1984. Early neurogenesis in wild-type *Drosophila melanogaster*. *Roux's Archives of Developmental Biology* 193, 308–325.

Heitzler, P., Simpson, P., 1991. The choice of cell fate in the epidermis of *Drosophila*. *Cell* 64, 1083–1092.

Henry, J.J., M.Q.M., 1999. Conservation and innovation in spiralian development. *Hydrobiologia* 402, 255–265.

Jacob, M.H., 1984. Neurogenesis in *Aplysia californica* resembles nervous system formation in vertebrates. *J. Neurosci.* 4, 1225–1239.

Jacobson, M., Rao, M.S., 2005. *Developmental Neurobiology*. Kluwer Academic/Plenum, New York.

Kadner, D., Stollewerk, A., 2004. Neurogenesis in the chilopod *Lithobius forficatus* suggests more similarities to chelicerates than to insects. *Dev. Genes Evol.* 214, 367–379.

Kramer, A.P., Weisblat, D.A., 1985. Developmental neural kinship groups in the leech. *J. Neurosci.* 5, 388–407.

Kunisch, M., Haenlin, M., Campos-Ortega, J.A., 1994. Lateral inhibition mediated by the *Drosophila* neurogenic gene delta is enhanced by proneural proteins. *Proc. Natl. Acad. Sci. U. S. A.* 91, 10139–10143.

Martin-Bermudo, M.D., Martinez, C., Rodriguez, A., Jimenez, F., 1991. Distribution and function of the lethal of scute gene product during early neurogenesis in *Drosophila*. *Development* 113, 445–454.

Mathis, L., Kulesa, P.M., Fraser, S.E., 2001. FGF receptor signalling is required to maintain neural progenitors during Hensen's node progression. *Nat. Cell Biol.* 3, 559–566.

Merkle, F.T., Alvarez-Buylla, A., 2006. Neural stem cells in mammalian development. *Curr. Opin. Cell Biol.* 18, 704–709.

Nielsen, C., 2004. Trochophora larvae: cell-lineages, ciliary bands, and body regions. 1. Annelida and Mollusca. *J. Exp. Zool. B Mol. Dev. Evol.* 302, 35–68.

Nieto, M., Schuurmans, C., Britz, O., Guillemot, F., 2001. Neural bHLH genes control the neuronal versus glial fate decision in cortical progenitors. *Neuron* 29, 401–413.

Pascale, A., Amadio, M., Quattrone, A., 2008. Defining a neuron: neuronal ELAV proteins. *Cell Mol. Life Sci.* 65, 128–140.

Pearson, B.J., Doe, C.Q., 2004. Specification of temporal identity in the developing nervous system. *Annu. Rev. Cell Dev. Biol.* 20, 619–647.

Robinow, S., White, K., 1991. Characterization and spatial distribution of the ELAV protein during *Drosophila melanogaster* development. *J. Neurobiol.* 22, 443–461.

Samson, M.L., 2008. Rapid functional diversification in the structurally conserved ELAV family of neuronal RNA binding proteins. *BMC Genomics* 9 (392).

Seaver, E.C., Kaneshige, L.M., 2006. Expression of 'segmentation' genes during larval and juvenile development in the polychaetes *Capitella* sp. I and *H. elegans*. *Dev. Biol.* 289, 179–194.

Seaver, E.C., Paulson, D.A., Irvine, S.Q., Martindale, M.Q., 2001. The spatial and temporal expression of Ch-en, the engrailed gene in the polychaete *Chaetopterus*, does not support a role in body axis segmentation. *Dev. Biol.* 236, 195–209.

Seaver, E.C., Thamm, K., Hill, S.D., 2005. Growth patterns during segmentation in the two polychaete annelids, *Capitella* sp. I and *Hydroides elegans*: comparisons at distinct life history stages. *Evol. Dev.* 7, 312–326.

Shankland, M., 1995. Formation and specification of neurons during the development of the leech central nervous system. *J. Neurobiol.* 27, 294–309.

Shook, D., Keller, R., 2003. Mechanisms, mechanics and function of epithelial-mesenchymal transitions in early development. *Mech. Dev.* 120, 1351–1383.

Simionato, E., Kerner, P., Dray, N., Le Gouar, M., Ledent, V., Arendt, D., Vervoort, M., 2008. atonal- and achaete–scute-related genes in the annelid *Platynereis dumerilii*: insights into the evolution of neural basic-Helix–Loop–Helix genes. *BMC Evol. Biol.* 8, 170.

Skeath, J.B., 1999. At the nexus between pattern formation and cell-type specification:

- the generation of individual neuroblast fates in the *Drosophila* embryonic central nervous system. *Bioessays* 21, 922–931.
- Skeath, J.B., Carroll, S.B., 1992. Regulation of proneural gene expression and cell fate during neuroblast segregation in the *Drosophila* embryo. *Development* 114, 939–946.
- Skeath, J.B., Thor, S., 2003. Genetic control of *Drosophila* nerve cord development. *Curr. Opin. Neurobiol.* 13, 8–15.
- Stollewerk, A., 2002. Recruitment of cell groups through Delta/Notch signalling during spider neurogenesis. *Development* 129, 5339–5348.
- Stollewerk, A., Simpson, P., 2005. Evolution of early development of the nervous system: a comparison between arthropods. *Bioessays* 27, 874–883.
- Stollewerk, A., Weller, M., Tautz, D., 2001. Neurogenesis in the spider *Cupiennius salei*. *Development* 128, 2673–2688.
- Thamm, K., Seaver, E.C., 2008. Notch signaling during larval and juvenile development in the polychaete annelid *Capitella* sp. I. *Dev. Biol.* 320, 304–318.
- Tomita, K., Moriyoshi, K., Nakanishi, S., Guillemot, F., Kageyama, R., 2000. Mammalian achaete–scute and atonal homologs regulate neuronal versus glial fate determination in the central nervous system. *EMBO J.* 19, 5460–5472.
- Torrence, S.A., Stuart, D.K., 1986. Gangliogenesis in leech embryos: migration of neural precursor cells. *J. Neurosci.* 6, 2736–2746.
- Turner, D.L., Weintraub, H., 1994. Expression of achaete–scute homolog 3 in *Xenopus* embryos converts ectodermal cells to a neural fate. *Genes Dev.* 8, 1434–1447.
- Urbach, R., Schnabel, R., Technau, G.M., 2003. The pattern of neuroblast formation, mitotic domains and proneural gene expression during early brain development in *Drosophila*. *Development* 130, 3589–3606.
- Wakamatsu, Y., Weston, J.A., 1997. Sequential expression and role of Hu RNA-binding proteins during neurogenesis. *Development* 124, 3449–3460.
- Yim, S.J., Lee, Y.S., Lee, J.A., Chang, D.J., Han, J.H., Kim, H., Park, H., Jun, H., Kim, V.N., Kaang, B.K., 2006. Regulation of ApC/EBP mRNA by the *Aplysia* AU-rich element-binding protein, ApELAV, and its effects on 5-hydroxytryptamine-induced long-term facilitation. *J. Neurochem.* 98, 420–429.
- Yoon, K., Gaiano, N., 2005. Notch signaling in the mammalian central nervous system: insights from mouse mutants. *Nat. Neurosci.* 8, 709–715.
- Younossi-Hartenstein, A., Nassif, C., Green, P., Hartenstein, V., 1996. Early neurogenesis of the *Drosophila* brain. *J. Comp. Neurol.* 370, 313–329.